UC Santa Barbara
UC Santa Barbara Electronic Theses and Dissertations

Title
A Thermoelectric Display for Assessment of Touch Sensory Deficits

Permalink
https://escholarship.org/uc/item/5571212q

Author
Patwardhan, Shriniwas Mahesh

Publication Date
2017

Peer reviewed|Thesis/dissertation

UNIVERSITY OF CALIFORNIA
Santa Barbara

A Thermoelectric Display for Assessment of Touch Sensory Deficits

A Thesis submitted in partial satisfaction
of the requirements for the degree of

Master of Science

in

Electrical and Computer Engineering

by

Shriniwas Patwardhan

Committee in Charge:

Prof. Yon Visell, Chair

Prof. João Hespanha

Prof. Brad Paden

June 2017

The Thesis of
Shriniwas Patwardhan is approved:

_____

Prof. João Hespanha

_____

Prof. Brad Paden

_____

Prof. Yon Visell, Committee Chairperson

June 2017

A Thermoelectric Display for Assessment of Touch Sensory Deficits

Acknowledgements

Abstract

A Thermoelectric Display for Assessment of Touch Sensory Deficits

Shriniwas Patwardhan

This thesis employed systems modeling and engineering design methods in order to study the 'thermal grill illusion' (TGI), a perceptual illusion in which a spatial configuration of warm and cool elements produce a paradoxical pseudo-burning sensation.

The motivation for this study was derived from the possibility to develop new methods for assessing peripheral sensory deficits affecting the sense of touch, associated with peripheral neuropathy. Thermal grill stimuli, consisting of spatial configurations of alternating warm and cool elements, are non-injurious and can elicit rapid and unambiguous perceptual responses, whose absence might provide a reliable indicator of sensory loss, although this has not been previously investigated, and is only indirectly addressed in this thesis.

An integrated custom electrothermal display was optimized for delivering thermal grill stimuli to the body. In order to validate the display technique, a thermodynamic model accounting for heat exchange (diffusion) through the skin was developed and the model predictions were compared with thermal perception.

I calibrated and assessed the approach in perceptual experiments with healthy human subjects.

Contents

List of Figures

xi

List of Tables

Chapter 1

Introduction

Information about an object's temperature and other thermal properties is sensed by our skin upon contact with that object. This makes thermal cues an important factor contributing to the differentiation of materials touched by the skin. The temperature of an object plays an important role in helping us determine the material of the object. For example, a wooden block and a metallic block, both kept out at room temperature will be at the same temperature after a certain amount of time, but the metallic block will feel colder. The reason for this is the difference in thermal conductivity of the material. Metals are better conductors than wood and hence they conduct the heat out of our hand when we touch them. This makes metals feel colder than wood. We use such knowledge about the thermal properties of an object to make perceptual judgments about

our environment. Thus, thermal feedback has become a point of study for those designing haptic displays. Haptic displays that employ interaction with a certain temperature or other thermal cue, are called thermal haptic displays and a typical thermal haptic display consists of one or many heating or cooling elements and a temperature measurement device [35].

In the field of haptics, we are interested in recreating perceptual experiences virtually using engineering techniques and a fine understanding of perception mechanisms in the human body. We are also interested in other applications which can benefit from the incorporation of thermal cues into the tactile feedback. By recreating the thermal characteristics of an object and the associated thermal sensations, a more realistic virtual representation of an object is possible. If we want to understand the thermal cues felt by the body during interaction, and recreate them, it is important to model the interaction between our body and thermal displays. This field of investigation inside haptics, describing the modeling, design and fabrication of thermal displays is called thermal display engineering.

This thesis aims to model the interaction between the body and a thermal haptic display, called the 'thermal grill'. A thermal grill is made up of a spatially alternating configuration of cool and warm stimuli, which give rise to a haptic illusion called 'thermal grill illusion'. Though these temperatures are not individually painful, touching a spatially alternating combination of mildly warm and

cool stimuli elicits a 'pseudo-burning' sensation. This thesis will investigate this haptic illusion, using systems modeling and engineering design approaches.

In this thesis, a thermal model has been proposed to describe the heat transfer in the skin during contact with the thermal grill. An understanding of how cutaneous tissues respond to thermal stimulation is needed for this purpose. This information is used to get a heat transfer model describing the propagation of heat through the skin. Once a heat transfer model is proposed, a haptic display capable of delivering the required thermal cues has been designed and fabricated, and the thermal response is predicted. The heat transfer problem has been solved analytically and numerically. A thermal grill display has been designed and fabricated in oder to elicit thermal grill illusion. An experimental study has been carried out in order to validate the model, by comparing the predicted thermal response of the skin to the experimental observations.

1.1   Biomedical Motivation - Assessment of Touch Sensory Deficits

The main motivation behind this thesis is the investigation into the detection of peripheral neuropathy using thermal displays. Peripheral neuropathy is a disease affecting the peripheral nerves, which damages them and affects the sensory

perception, shifting the threshold of pain such that normal levels of pain feel either too painful or not painful at all. There has been a recent interest among health care professionals to find quick, reliable and portable ways to detect neuropathy. Neuropathy is associated with symptoms such as burning pain, paraesthesia, hyperesthesia and painful cramps. Neuropathy patients complain about decreased tactile sensation and drastic changes in thermal perception [23]. Current methods of detecting neuropathy involve EMG and nerve conduction tests.

But EMG and NC techniques evaluate large sensory nerve fiber function (responsible for detecting mechanical stimuli) and not small sensory nerve fiber function (responsible for sensing heat, cold and pinch). Small sensory nerve fiber function is altered earlier than large sensory nerve fiber function in neuropathy patients [23]. Thus, it would be advantageous to make use of another technique which focuses dominantly on small sensory nerve fibers, so that early detection of sensory loss in neuropathy patients can be achieved.

Although 'thermal or painful tactile stimuli' are ideal for stimulating small sensory nerve fibers and hence for detecting loss of sensation, such stimuli can elicit discomfort and even damage the tissues. Hence, we propose a method to detect neuropathy should with following characteristics.

1. It should induce a thermal stimulus.

2. It should elicit a quick and unambiguous sensation and response.

3. It should not cause any actual harm or pain.

4. It should be non-invasive (i.e. not tending to infiltrate and destroy healthy tissue).

5. It should stimulate the small sensory nerve fibers in a targeted manner rather than the long sensory nerve fibers.

Such a stimulus is available in the thermal grill illusion.

1.2   Main Research Question

In order to investigate the effectiveness of TGI to assess sensory deficits, it is crucial to quantitatively study the effect elicited by it. Prior literature indicates that the strength of the illusion depends on the warm-cool differential, but the temporal properties have not been previously studied.

In this thesis, I investigate the thermal grill illusion and quantitatively assess the response elicited by it. I study the variation in response time (time taken by the body after touching the thermal grill before it causes a burning sensation), with a variation in the warm-cool differential of the thermal grill. I hypothesize that a higher differential should then lead to a quicker response, lowering the response time. To quantitatively assess the effect of the thermal grill illusion, a

thermodynamic model is needed, which can predict the time-dependent response elicited by it.

1.3   Contributions of this Thesis

The novel aspects of this thesis involve the study of response time to the thermal grill illusion. Thermodynamic modeling provided a framework to predict the response elicited by the thermal grill. The perceptual experiment results were compared to the modeling results and a preliminary comparison could be conducted. The main contributions of this thesis are as follows.

1. Design, fabrication and implementation of a thermal haptic display, called the thermal grill. This device is capable of setting the temperatures of the thermal grill at the desired levels. It is also capable of measuring the participant's response time to the thermal grill illusion. The measurement of response time to the thermal grill illusion is a novel contribution of this thesis.

2. Formulation of a thermodynamic model describing time-dependent interaction between the thermal grill and the cutaneous body tissues and development of analytical and numerical solutions describing the thermodynamics of body tissues stimulated by a thermal grill.

3. Comparison of perceptual responses to the thermal grill illusion recorded during the experiment to the predicted thermodynamics of tissue heating.

4. Experimental study investigating the effect of temperature differential of the thermal grill on the response elicited by it. Specifically, we measure and investigate the dependence of response time on the temperature difference, in order to compare with the time-variation of temperature gradients predicted by the thermal model.

This thesis contributes to the area of human haptics, which is the study of human sensing through touch, and more precisely to the sub-area of cutaneous sensing. By modeling the heat transfer when in contact with the body, it also contributes to the area of thermal sensation and thermal display engineering.

1.4   Organization of the Thesis

The thesis is organized into five chapters: this introduction and four more chapters which are as follows.

Chapter 2 gives a detailed summary of background literature available in the area of modeling of thermal displays. It then goes on to explain thermal grill illusion in detail and explores the multiple causes of thermal grill illusion proposed in the literature.

Chapter 3 proposes a thermodynamic model to explain the thermal grill illusion. We split the problem into two parts - steady state and transient, and then propose a solution for each of them. We solve the heat diffusion problem analytically and numerically and discuss the solutions in chapter 3.

Chapter 4 describes the experimental study carried out to validate the model described in chapter 3. We asked the subjects of the experiment to feel the thermal grill at various temperature settings and recorded their responses. These were the response time and perceived intensity. We compared the results of our experimental study with the predictions of our thermodynamic model.

Chapter 5 examines the main findings of the thesis and lists the conclusions from them.

Chapter 2

Background

A thermal haptic display is a device that incorporates thermal feedback using one or more temperature-controlled elements, allowing the user to feel the various thermal cues of a perceived object, thereby providing a richer tactile experience. A typical thermal haptic display consists of one or many heating or cooling elements and a temperature measurement device [35]. Prior research [24] suggests that thermal cues play a crucial role in material discrimination. Hence, if we want to understand the haptic cues felt by the body during interaction, and recreate them virtually, it is important to model the interaction between our body and thermal displays. The thermal cues that help the body understand the thermal properties of the objects while interacting with them are largely derived from the change in temperature of the skin upon contact with the object [25]. Modeling

the interaction between the human body and the thermal displays is vital to understanding the underlying physical mechanisms which give rise to thermal perception.

2.1   Modeling dynamics of thermal displays

Several authors have discussed heat diffusion in body tissues and related aspects of thermal display design [40]. The argument has been posed that the human finger is a multi-layered complex system made up of multiple individual tissues and interacting solid and fluid components. Apart from this, there is also the question of thermal damage and breakdown. When the body tissues are subjected to temperatures beyond the physiological temperature limits, it ultimately causes tissue damage. This system is further complicated by the involvement of blood vessels in the vascular network which act as conduits for heat transfer from one tissue to the other parts of the body. There is also the complexity of accounting for the heat transfer carried out by the skin blood perfusion [40].

A starting point for modeling thermal displays that are in contact with body tissues is based on the bioheat equation [37]. It was the first model that quantified the heat transfer effect of blood perfusion, see Equation (2.1). The bioheat transfer equation describes the thermal behavior based on the classical Fourier law and is based on the assumption that all heat transfer occurs in the capillaries. The
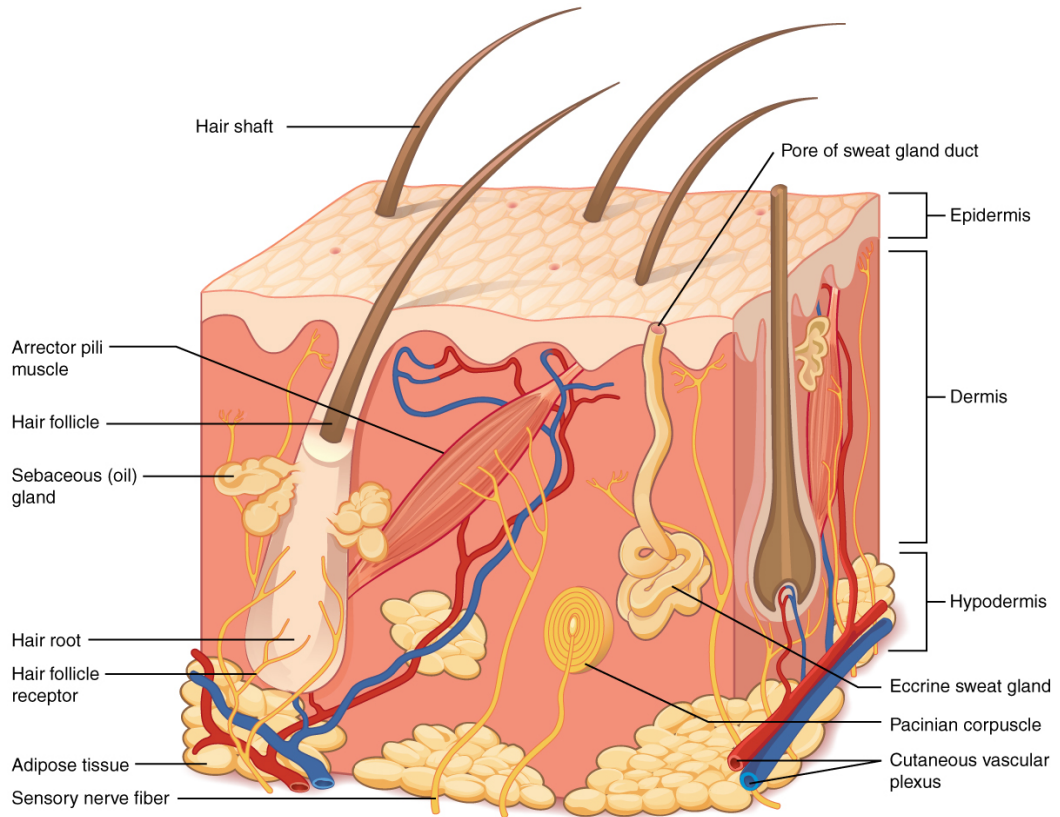
Figure 2.1: A diagram showing different layers of the skin such as epidermis, dermis and hypodermis. The thickness of these layers varies for different body parts. This figure has been reproduced from [8]

bioheat equation is given by

$$\rho c \frac{\partial T}{\partial t} = k \nabla^2 T + \omega_b \rho_b c_b (T_a - T) + q_{met} + q_{ext} \qquad (2.1)$$

where ρ, c and k are the density, specific heat and thermal conductivity of skin tissue, respectively; ρ_b and c_b are the density and specific heat of blood as before;

ω_b is the blood perfusion rate per unit volume; T_a and T are the temperatures of blood and skin tissue, respectively; q_{met} is the metabolic heat generation in the skin tissue and q_{ext} is the heat generation due to external heating sources. This model adds a blood perfusion term to account for the heat transfer due to the blood and it is linear with respect to temperature. Pennes' model is widely used for prediction of temperature elevation during hyperthermia [40].

Benali-Khoudjal [3] used an electrical analogy to explain the interaction, but it is not a common approach.

Jones and Ho [20] [21] proposed a thermal model that predicts the temperature responses of the skin and material surface during hand-object interactions. Their model accounts for the heat flux exchanged during interaction with an object. They accounted for the thermal contact resistance by measuring the surface features of the finger pad. They performed simulations to calculate the thermal responses of the finger pad as it made contact with a material. A semi-infinite body model was used for this purpose. Their findings indicated that the inclusion of the thermal resistance in the model gives a more complete picture of the thermal responses of the hand and hence gives us more accurate time constants of thermal responses.

The model described by Jones and Ho [20] [21] is given by

$$T_{skin,s}(t) = \frac{A}{B}\left[1 - e^{\alpha_{skin}B^2 t} erfc\left(B\sqrt{\alpha_{skin}t}\right)\right] + T_{skin,i} \qquad (2.2)$$

where

$$A = \frac{-(T_{skin,i} - T_{object,i})}{k_{skin}R}$$

$$B = \frac{1}{k_{skin}R}\left[1 + \frac{(k\rho c)^2_{skin}}{(k\rho c)^2_{object}}\right]$$

$$T_{object,s}(t) = \frac{C}{D}\left[1 - e^{\alpha_{object}D^2 t}erfc\left(D\sqrt{\alpha_{object}t}\right)\right] + T_{object,i} \qquad (2.3)$$

where

$$C = \frac{(T_{skin,i} - T_{object,i})}{k_{object}R}$$

$$D = \frac{1}{k_{object}R}\left[1 + \frac{(k\rho c)^2_{object}}{(k\rho c)^2_{skin}}\right]$$

where k is the thermal conductivity, ρ is the density, c is the specific heat capacity, and α is the thermal diffusivity. The surface temperatures of the skin and object are given as $T_{skin,s}$ and $T_{object,s}$. This model does not describe the behavior as a function of depth inside the skin or position along it. It gives the temperature of the object and the skin at the surface, at the point of contact, but does not tell us how the thermal response evolves over time inside the body at a certain depth. We are more interested in the thermal response at a depth because we would like to incorporate the response of the thermoreceptors into the model.

We are not only interested in modeling the interaction between the human body and a thermal display but a specific thermal haptic illusion.

2.2   Tactile Illusions

Haptic illusions are an inconsistency between a physical stimulus and its perception. In general, haptic illusions can be only tactile (involving sense of touch) [22] or involve multi-modal stimulation of the sensory channels such as audio, visual and touch [5][27]. Tactile illusions are the illusions that involve the sense of touch, and work the same way as do illusions of other senses like smell, vision and audio. Even though the number of tactile illusions described in the literature is small as compared to the illusions of other senses, there is a large body of literature describing tactile illusions [18][29][34]. Haptic illusions give us a deeper insight into the perceptual process by which we feel the environment around us and can also be used in application such as robot assisted surgery by supplying haptic feedback to the surgeon's hands [36].

Thermal sensing is a crucial component which contributes to our understanding of our environment, along with the massive amount of information we gain from our skin. We combine this information with other features like surface roughness in order to perceive the objects we touch.

In this thesis, we have used a thermal tactile illusion called the thermal grill illusion and we have made a custom thermoelectric haptic display to create this illusion.

2.3   Thermal Grill Illusion

The thermal grill illusion is a haptic illusion that was discovered by Torsten Thunberg. In 1896, Thunberg reported that innocuous warm and cool stimuli applied simultaneously to the skin by means of interlocking spiral tubes elicited a sensation of strong heat, which he compared to the burning sensation that commonly accompanies cold pain [39]. The illusion can also be experienced by using shapes other than spiral tubes.

(a) Only warm bars   (b) Only cool bars   (c) Thermal Grill
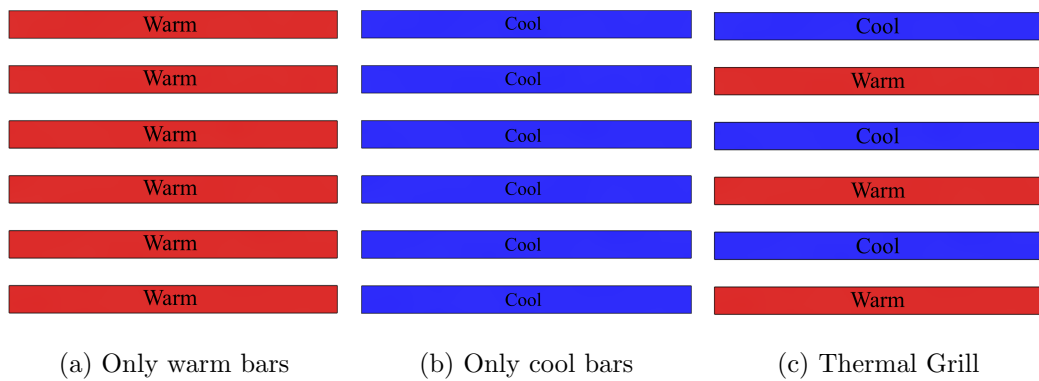
Figure 2.2: Spatially spaced out warm bars feel warm, spatially spaced out cool bars feel cool, but spatially alternating warm and cool bars (thermal grill) feel burning hot.

Some examples of shapes used for making a thermal grill include alternating bars, checkerboard patterns and spaced out dots arranged in a grid-like-pattern. It has been shown in a study [31], the occurrence of the thermal grill illusion does

not show significant change with changing the number of stimuli or the distance between them. The strength of the illusion drops off considerably after a certain threshold specific to the shape of the display, but stays mostly regular within those limits.

The normal temperature of human skin is between $31 - 35°$C. Temperatures above that are perceived as warm, and temperatures above $45-47°$C are perceived as painfully hot. Temperatures below the body temperature are perceived as cool, and temperatures below $12 - 15°$C are perceived as painfully cold. There are distinct classes of thermoreceptors in the skin corresponding to these temperature ranges [10]. The thermoreceptors, that are temperature sensitive afferent nerve fibers translating temperature information into neural information, respond normally to temperatures between $15-45°$C but the body perceives pain immediately above and below these temperatures [38] [13].

The thermal grill does not expose the skin to temperatures that are in the painful range given above. The illusion is a paradoxical sensation of burning, because touching only the cold or hot bars individually does not induce the same level of discomfort. If the individual touches only the warm bars, only warmth is experienced while touching only the cold bars feels cool [2]. The temperature of the skin clearly does not reach the painful levels described in the literature and yet there is an unambiguous and quick response to the thermal grill. For example, in

a study conducted by Lindstedt, et al. [32], it was shown that the the thermal grill illusion was rated as significantly more unpleasant and painful than stimulation with each of its individual constituent temperatures.

Several explanations have been proposed for the thermal grill illusion. In the early part of the 19th century, a theory of pain 'fusion' was put forth. According to this theory, the explanation of the thermal grill illusion is based on Alrutz's proposal that the perception of 'heat' (evoked at temperatures above 45°C) is not a specific sensation but rather a fusion resulting from the simultaneous activation of specific warm and cold spots [4]. Later experimental findings about the discharge of thermoreceptors have contradicted this theory.

A more sophisticated explanation, namely the 'disinhibition theory' was proposed by Craig and Bushnell [12]. They investigated the cause of the thermal grill illusion using neurophysiological and psychophysical methods. Thunberg had argued that a selective block of the sensory channel for warmth would enable a hot stimulus to elicit a cold sensation [39], but in fact the opposite occurred. If you remove the person's sensibility to cold but not to warmth, it actually enabled a cold stimulus to elicit a burning heat sensation [28]. They hypothesized that the response to the thermal grill is due to the central unmasking of the cold-activated C polymodal nociceptive channel [11]. They proposed a simple integrative model that could explain the grill illusion. Thus, their findings indicate that the ther-

mal grill illusion is a central disinhibitory phenomenon in which the reduction of inhibition induced by the cold channel exposes (or unmasks) the cold-sensitive activity, thereby evoking the burning hot pain felt when touching the grill [11].

Evans and Bushnell [9] localized the thermal grill illusion and the underlying unmasking mechanism in the human brain, using a technique called 'Positron Emission Tomography' (PET). They compared the activity in the cortical region of the brain by observing the patterns evoked by the thermal grill and cool, warm, noxious cold and noxious hot heat stimuli. Their results showed that the thermal grill and the noxious hot and cold stimuli produce activation in the anterior cingulate cortex whereas the warm and cool components of the thermal grill do not.

2.4 Biomedical motivation for using TGI for detecting touch sensory deficits

Neuropathy is a condition of the nervous system in which the sensory capacities of the bod are hampered by lowering or heightening the threshold for pain. Alarmingly, 30 % of hospitalized and 20 % of community-dwelling diabetes patients have peripheral neuropathy and 2 % cases show fatality, annually [15]. Out of all the diabetes patients, 4-15 % of diabetes mellitus patients show a tendency

to develop neuropathy. Some patients show clear symptoms while some do not. The most common form of neuropathy are chronic sensorimotor distal symmetric polyneuropathy, which gives rise to numbness, tingling, pain, and weakness starting in the toes. In symptomatic patients, mechanical methods allow clinical diagnosis of distal symmetrical polyneuropathy (DSPN) in 87 % of the cases, while in asymptomatic patients, mechanical methods may under diagnose 85-96 % of these patients [7]. To overcome the problem of under-diagnosis, electromyography (EMG) and nerve conduction (NC) [16] are the most used techniques to quantify nerve damage [7] [30] [14]. But EMG and NC are difficult to apply. During an EMG test, the needle electrode is put into a muscle. After the test, patients may be sore and feel pain in the muscles, which may last for days. These methods are therefore not suitable for old patients and those with acute sensory dysfunction. Health care professionals hence find EMG and NC to be too invasive and bulky, in order to prescribe regularly.

More importantly, EMG and NC techniques evaluate large sensory nerve fiber function and not small sensory nerve fiber function. Small sensory nerve fiber function is altered earlier than large sensory nerve fiber function in neuropathy patients [23]. Thus, it would be advantageous to make use of another technique which focuses dominantly on small sensory nerve fibers, so that early detection

of sensory loss in neuropathy patients can be achieved. Small fiber function is involved in autonomic function, sensing of cold, heat, and pain.

Although painful thermal or tactile stimuli would be ideal for stimulating small sensory nerve fibers and hence for detecting loss of sensation, such stimuli can elicit discomfort. More importantly, they are also associated with tissue damage. In addition, the assessment of thermal thresholds is time consuming and bias prone.

Chapter 3

Thermal Modeling of the

Thermal Grill Illusion

This chapter aims to model the interaction of the hand's skin and the thermal grill by finding a spatiotemporal solution to the heat diffusion equation by applying the boundary conditions imposed by the thermal grill. For this purpose we propose a spatiotemporal model that describes the propagation of heat through the skin when the hand touches the thermal grill.

The complex nature of the heat diffusion problem applied to the finger makes it difficult to account for all the heat sources and sinks adequately. We propose a model that assumes that the finger is made up of a homogeneous material of thermal conductivity k_{finger}. For simplicity, this model will not take into account

the skin blood perfusion, thermal breakdown and damage to the skin, and the

internal workings of the skin tissue.

3.1   Physical Modeling
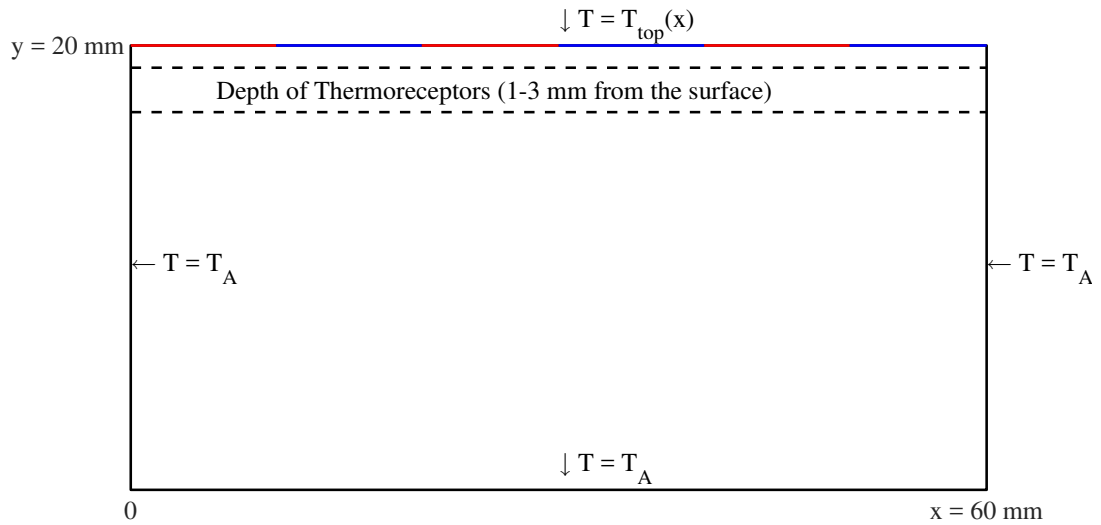
Figure 3.1: Boundary conditions for hand touching thermal grill. The top bound-

ary is the thermal grill whereas the other three are held at ambient body temper-

ature.

We are interested in finding the solution to the heat diffusion equation over

the domain corresponding to the volume of tissue near the surface of the skin. We

will be solving to find a time dependent analytical solution to the heat diffusion

equation given by

$$\frac{\partial^2 T(x,y,t)}{\partial x^2} + \frac{\partial^2 T(x,y,t)}{\partial y^2} = \frac{1}{k_{finger}} \frac{\mathrm{d}T(x,y,t)}{\mathrm{d}t} \qquad (3.1)$$

	X-axis	Y-axis	Temperature
Left Boundary	$x = 0$	$0<y<b$	$T(x,y,t) = T_A$
Right Boundary	$x = a$	$0<y<b$	$T(x,y,t) = T_A$
Bottom Boundary	$0<x<a$	$y = 0$	$T(x,y,t) = T_A$
Top Boundary	$0<x<a$	$y = b$	$T(x,y,t) = T_{top}(x)$

Table 3.1: Boundary conditions for heat equation over the domain corresponding to the volume of body tissue near the surface of the skin

The top side is held at the temperature of the thermal grill. This is $T_{top}(x)$. This is the temperature profile corresponding to the hot and cold temperatures actually used on the thermal grill. The bottom, left and right boundary are maintained at ambient body temperature (T_A). As T_A is a constant and we are solving a linear differential equation, we can subtract T_A form all the sides and define a new set of boundary conditions. Now, after subtracting T_A from all sides, the new boundary conditions become 0 on the left, bottom and right boundary and $T_{TGI}(x) = T_{top}(x) - T_A$ on the top boundary.

	X-axis	Y-axis	Temperature
Left Boundary	$x = 0$	$0<y<b$	$T(x, y, t) = 0$
Right Boundary	$x = a$	$0<y<b$	$T(x, y, t) = 0$
Bottom Boundary	$0<x<a$	$y = 0$	$T(x, y, t) = 0$
Top Boundary	$0<x<a$	$y = b$	$T(x, y, t) = T_{TGI}(x)$

Table 3.2: Boundary conditions for heat equation over the domain corresponding to the volume of body tissue near the surface of the skin after subtracting ambient body temperature from all the sides

Now, we want to solve Equation (3.1) for the boundary conditions given in Table (3.2). The top boundary is thermal grill after subtracting the ambient body temperature. The hot temperature is denoted as T_{hot} and the cold temperature as T_{cold}. The temperature profile of the top surface is then a square wave with value $\pm T_{hot}$.
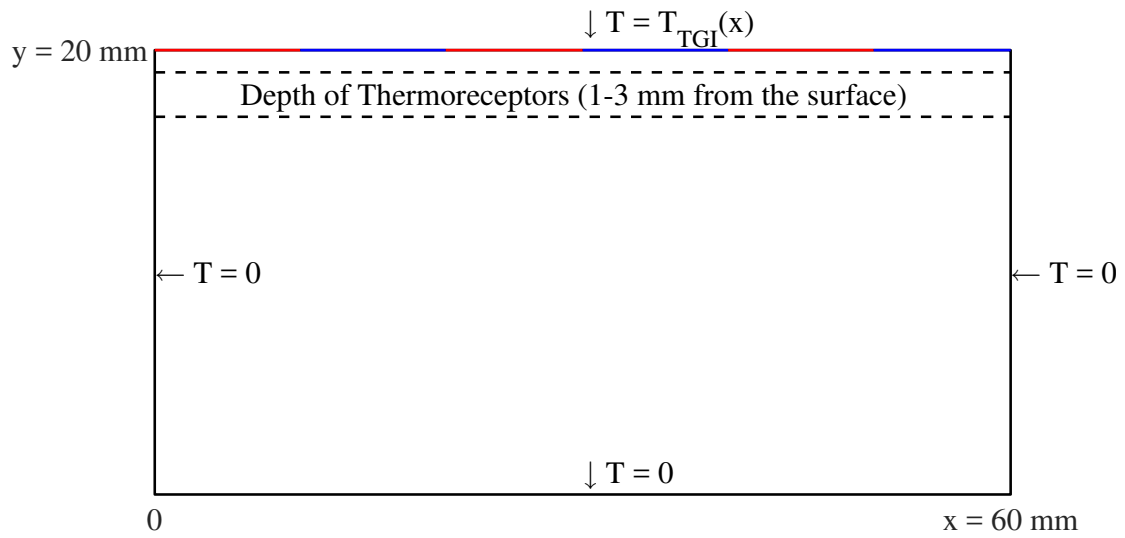
Figure 3.2: Boundary conditions for hand touching thermal grill. The top boundary is the thermal grill after subtracting ambient body temperature whereas the other three sides are shown to be at $T = 0$
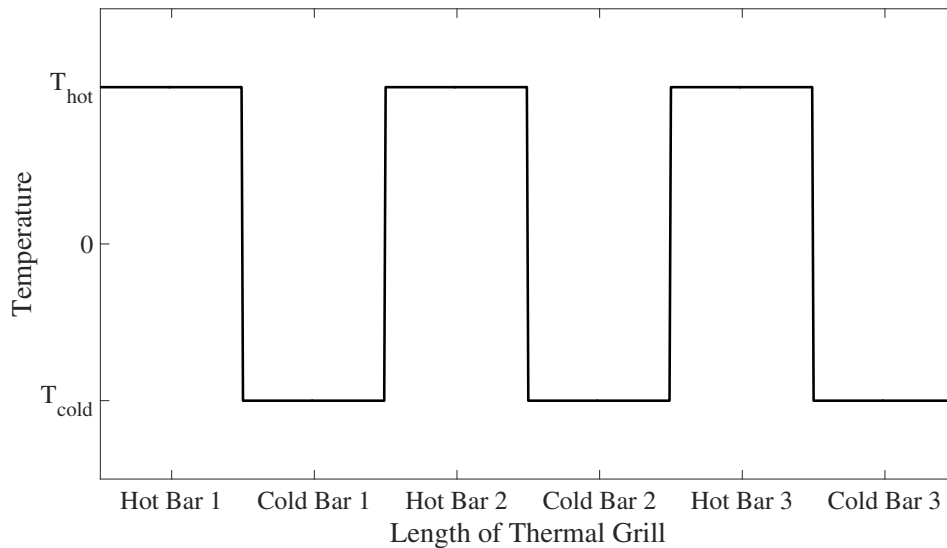
Figure 3.3: Temperature profile for thermal grill, shown using a square wave of amplitude $\pm T_{hot}$

25
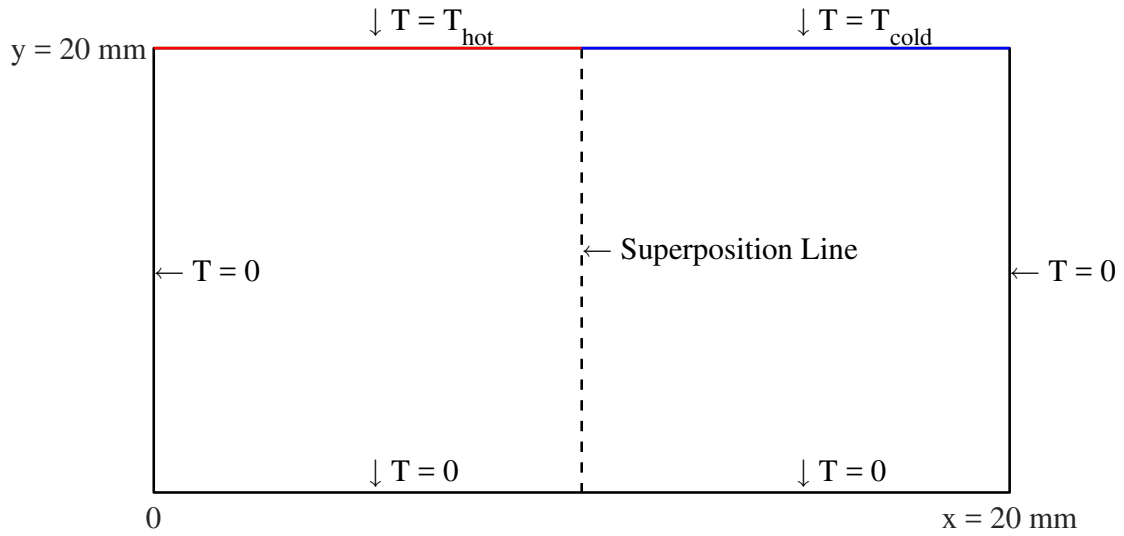
Figure 3.4: Boundary conditions for one Hot-Cold pair of temperatures

First, we will decompose the thermal grill given by multiple hot-cold pairs into pairs and then investigate only one pair at a time. The resultant effect of all of them must be a linear combination of all such pairs, see Figure (3.4).

3.1.1   Time-dependent solution by superposition

Let D be a linear differential operator, let f_1 and f_2 be functions and let c_1 and c_2 be constants.

- If u_1 solves the linear partial differential equation $Du = f_1$ and u_2 solves the linear partial differential equation $Du = f_2$, then $u = c_1 u_1 + c_2 u_2$. In

particular, if both solve the same homogeneous linear partial differential equation, then so does $u = c_1 u_1 + c_2 u_2$.

- If u_1 satisfies the linear boundary condition $Du|_A = f_1|_A$ and u_2 satisfies the linear boundary condition $Du|_A = f_2|_A$, then $u = c_1 u_1 + c_2 u_2$ satisfies $Du|_A = c_1 f_1 + c_2 f_2|_A$. In particular, if u_1 and u_2 both satisfy the same homogeneous linear boundary condition, so does $u = c_1 u_1 + c_2 u_2$.

We first consider the problem given in Figure (3.4).The solution along the dashed line will be $T(x, y, t) = 0$ provided that the initial condition is also $T_0(x, y, 0) = 0$. We can now show that the problem given in Figure (3.4) can be shown as the result of superposition of the two problems given in Figure (3.5a) and Figure (3.5b).

If $T_1(x, y, t)$ is the solution when the top boundary condition is $(T, 0)$ and $T_2(x, y, t)$ is the solution when the top boundary condition is $(0, -T)$, then we can see that the two solutions are related by reflection about the dashed line and a multiplication factor of -1. Now along the dashed line, we will have the following. T_{hot} and T_{cold} are related as $T_{hot} = -T_{cold}$.

$$T_1(\frac{a}{2}, y, t) = -T_2(\frac{a}{2}, y, t) = 0$$
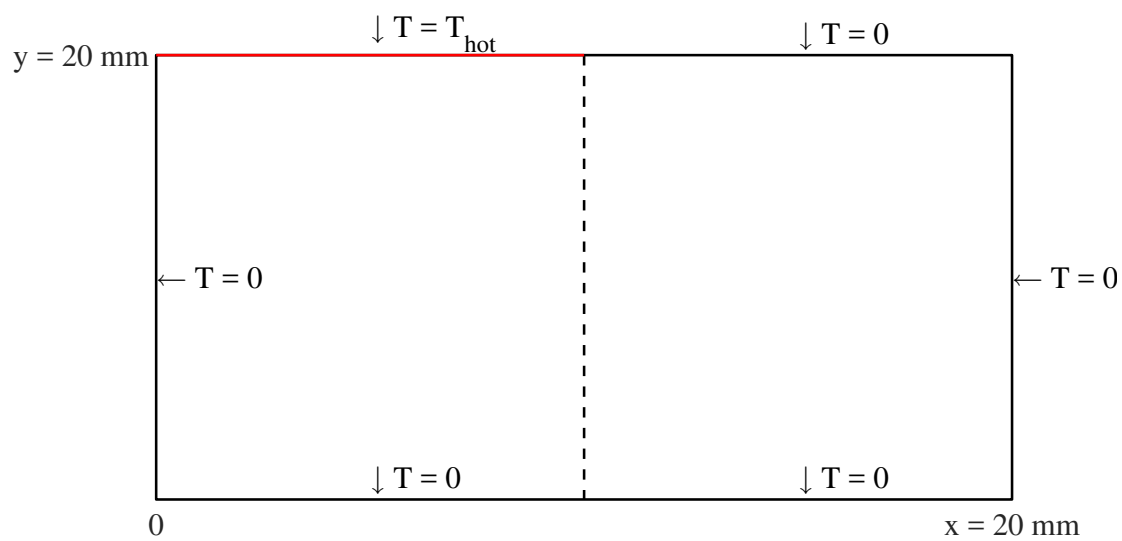
(a) Problem 1 : Boundary conditions in the presence of only T_{hot}
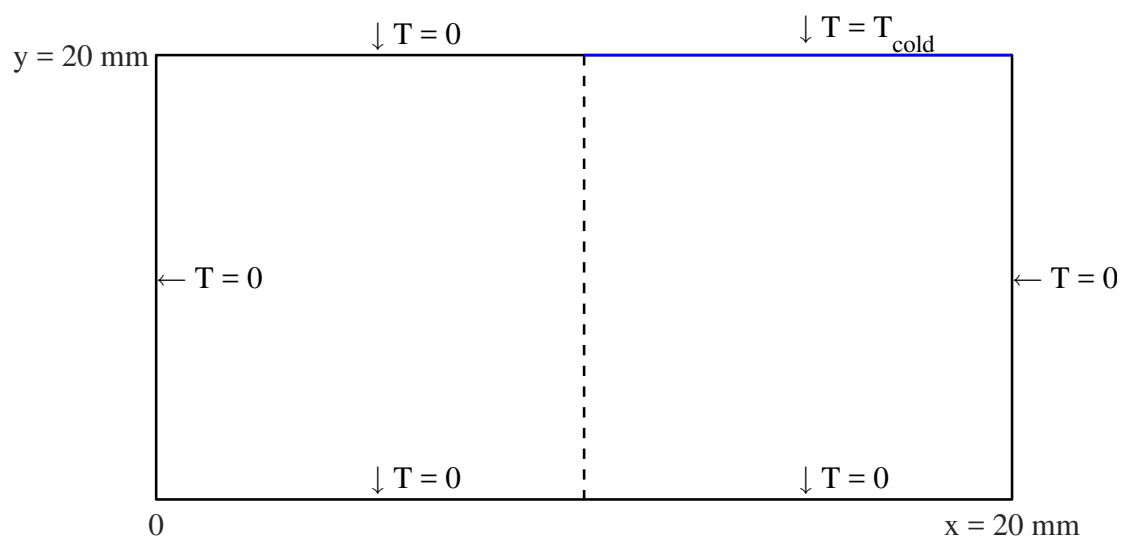
(b) Problem 2 : Boundary conditions in the presence of only T_{cold}

Figure 3.5

We can hence consider the problem given in Figure (3.4). The solution to the left side of the dashed line will be the solution to the time-dependent problem with boundary conditions $(T_{hot}, 0, 0, 0)$ and the solution to the right side will be the solution to the time-dependent problem with boundary conditions $(T_{cold}, 0, 0, 0)$, which is the same as $(-T_{hot}, 0, 0, 0)$. The heat diffusion in the rectangular area is governed by linear differential equations whose solution depends on the boundary conditions.

Thus, for the general problem of the thermal grill, it is sufficient to solve the problem given in Figure (3.6). This reduces the complexity of the problem by letting us solve the problem given in Figure (3.6).

We can break down the problem into its steady state and transient components and solve each individually. Let $T_{ss}(x, y)$ be the steady state solution and $T_t(x, y, t)$ be the transient part of the solution. The complete solution will then be $T(x, y, t) = T_{ss}(x, y) + T_t(x, y, t)$.

3.1.2   Steady State Solution

The horizontal direction is taken to be x and the vertical direction is taken to be y. The thermal conductivity is assumed to be constant and equal to that of the skin at the surface ($k = k_{skin} = k_{finger}$).

	X-axis	Y-axis	Temperature
Left Boundary	$x = 0$	$0<y<b$	$T(x,y,t) = 0$
Right Boundary	$x = a$	$0<y<b$	$T(x,y,t) = 0$
Bottom Boundary	$0<x<a$	$y = 0$	$T(x,y,t) = 0$
Top Boundary	$0<x<a$	$y = b$	$T(x,y,t) = T_{hot}$ or T_{cold}

Table 3.3: Boundary conditions for Heat Equation (part-wise)
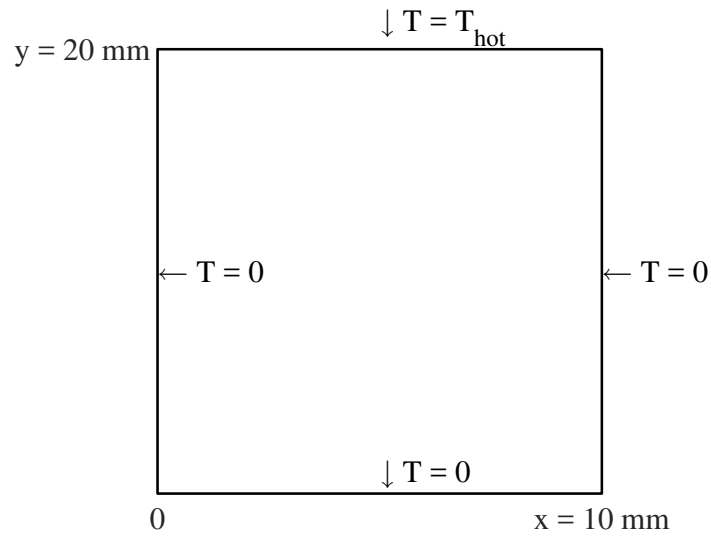
Figure 3.6: Boundary conditions for a single element, where T_s is the temperature of the top boundary. This can be either T_{hot} or T_{cold}

$$k = k_{finger} \qquad \forall \qquad \{x,y|0 < x < a \text{ and } 0 < y < b\}$$

The finger is initially held at a temperature $T_0(x, y)$.

$$T(x, y, t = 0) = T_0(x, y)$$

After $t = 0$, the rectangle is heated from the top side, and the remaining sides are maintained at the $T = 0$. The temperature of the heating element is held at $T = T_{hot}$.

This problem will be solved in two parts. First we will find the steady state solution to this problem, and then proceed to finding the transient solution. The first part of the problem is to calculate the steady state solution $T(x, y) = \lim_{t \to \infty} T(x, y, t)$. This in a standard heat transfer problem, with a well-known solution [17], when the temperature of the boundaries is held at known values. It satisfies the heat equation, but because there is no time dependence, the time derivative goes to 0 and we are left with only the terms given by

$$\frac{\partial^2 T}{\partial x^2} + \frac{\partial^2 T}{\partial y^2} = 0 \qquad (3.2)$$

To use the method of separation of variables, we assume that the function $T(x, y)$, which is the steady state solution of our problem can be expressed as the product of a function in only x, $f(x)$ and a function in only y, $g(y)$.

$$T(x, y) = f(x).g(y) \qquad (3.3)$$

Substituting this in Equation (3.2),

$$g(y)\frac{\mathrm{d}^2 f(x)}{\mathrm{d}x^2} + f(x)\frac{\mathrm{d}^2 g(y)}{\mathrm{d}y^2} = 0$$

$$\frac{-1}{f(x)}\frac{\mathrm{d}^2 f(x)}{\mathrm{d}x^2} = \frac{1}{g(y)}\frac{\mathrm{d}^2 g(y)}{\mathrm{d}y^2} \qquad (3.4)$$

Both sides of Equation (3.4) are functions of different independent variables. In this case, both sides will have to be equal to a constant for them to be equal to each other and the equality to hold.

$$\frac{\mathrm{d}^2 f(x)}{\mathrm{d}x^2} + \lambda^2 f(x) = 0$$
$$\frac{\mathrm{d}^2 g(y)}{\mathrm{d}y^2} - \lambda^2 g(y) = 0$$

which have the following solution.

$$f(x) = B\cos(\lambda x) + C\sin(\lambda x)$$

$$g(y) = De^{-\lambda y} + Ee^{\lambda y}$$

$$T(x,y) = f(x) \cdot g(y) = [B\cos(\lambda x) + C\sin(\lambda x)]\left[De^{-\lambda y} + Ee^{\lambda y}\right] \qquad (3.5)$$

Now, we shall apply the boundary conditions.

Boundary Condition 1 : $x = 0$ and $0 < y < b$

$$B(De^{-\lambda y} + Ee^{\lambda y}) = 0$$

$$B = 0$$

Boundary Condition 2 : $y = 0$ and $0 < x < a$

$$C \sin(\lambda x)(De^0 + Ee^0) = 0$$

$$D = -E$$

Boundary Condition 3 : $x = a$ and $0 < y < b$

$$CD \sin(\lambda a)(e^{-\lambda y} - e^{\lambda y}) = 0$$

$$-2CD \sin(\lambda a) \sinh(\lambda y) = 0$$

Boundary condition 3 requires $\sin(\lambda a) = 0$, which has roots $\lambda_n = \frac{n\pi}{a}$, for $n = 0, 1, 2, \dots$.

Now, let $-2CD = A_n$.

$$T_n(x, y) = A_n \sin \frac{n\pi x}{a} \sinh \frac{n\pi y}{a} \qquad\qquad n = 0, 1, 2.3... \qquad (3.6)$$

Equation (3.2) is a linear differential equation. Hence, the solution is the sum of all solutions given by Equation (3.6).

$$T(x, y) = \sum_{n=1}^{\infty} A_n \sin \frac{n\pi x}{a} \sinh \frac{n\pi y}{a} \qquad\qquad (3.7)$$

Boundary Condition 4 : $y = b$ and $0 < x < a$

$$T_s = \sum_{n=1}^{\infty} A_n \sin \frac{n\pi x}{a} \sinh \frac{n\pi b}{a}$$

If the distribution of temperature along the boundary $y = b$ is given by some function $w(x)$.

$$f(x) = \sum_{n=1}^{\infty} C_n \sin \frac{n\pi x}{a} \quad ; \quad C_n = A_n \sinh\left(\frac{n\pi b}{a}\right) \tag{3.8}$$

To get constants C_n, multiply Equation (3.8) by $\sin \frac{n\pi x}{a}$ and integrate term by term from $x = 0$ to $x = a$.

$$\int_0^a w(x) \sin\left(\frac{n\pi x}{a}\right) dx = \int_0^a C_1 \sin\left(\frac{\pi x}{a}\right) \sin\left(\frac{n\pi x}{a}\right) dx + \dots$$

$$+ \int_0^a C_n \sin\left(\frac{n\pi x}{a}\right) \sin\left(\frac{n\pi x}{a}\right) dx +$$

$$\dots + \int_0^a C_m \sin\left(\frac{m\pi x}{a}\right) \sin\left(\frac{n\pi x}{a}\right) dx \tag{3.9}$$

$$\int_0^a \sin\left(\frac{n\pi x}{a}\right) \sin\left(\frac{m\pi x}{a}\right) dx = 0 \qquad \text{for } n \neq m$$

$$\int_0^a \sin^2\left(\frac{n\pi x}{a}\right) dx = \frac{a}{2n\pi}\left[\frac{n\pi x}{a} - \frac{1}{2}\sin\left(\frac{2n\pi x}{a}\right)\right]_0^a = \frac{a}{2}$$

$$C_n = \frac{2}{a} \int_0^a w(x) \sin \frac{n\pi x}{a} \, dx \tag{3.10}$$

For the function $w(x)$ equal to a constant value T_s,

$$C_n = \frac{2}{a}\left[\frac{-T_s a}{n\pi} \cos\left(\frac{n\pi x}{a}\right)\right]_0^a = T_s \frac{2}{n\pi}\left[1 - (-1)^n\right]$$

We can calculate A_n as given in Equation (3.11).

$$A_n = \frac{C_n}{\sinh(n\pi b/a)} = \frac{2\left[1 - (-1)^n\right]}{n\pi \sinh(n\pi b/a)} \tag{3.11}$$

$$T(x,y) = T_s \sum_{n=1}^{\infty} \frac{2\left[1 - (-1)^n\right]}{n\pi \sinh(n\pi b/a)} \sin\left(\frac{n\pi x}{a}\right) \sinh\left(\frac{n\pi y}{a}\right) \tag{3.12}$$

Equation (3.12) gives the steady state temperature distribution $T(x,y)$ at any horizontal point x and depth y. This will give us the solution over one domain.

As explained before, this piecewise solution can be put together side by side and solved for $\pm T_{hot}$ to get the solution for the full thermal grill. As the boundary between two cells will always remain at $T = 0$, which are the boundary conditions for the adjacent cell, individual solutions to $\pm T_{hot}$ ca be computed separately and placed in next to each other horizontally in order to get the full solution. The steady state solution has been computed numerically, for a sample $T_{TGI}(x)$ alternating between $\pm 25°C$.

The solution given in Figure (3.7) gives the entire solution corresponding to the entire area being touched by the thermal grill. This is computed by placing the piece-wise individual solutions next to each other. A example of such a constituent solution has been shown using the red dotted line in Figure (3.7)
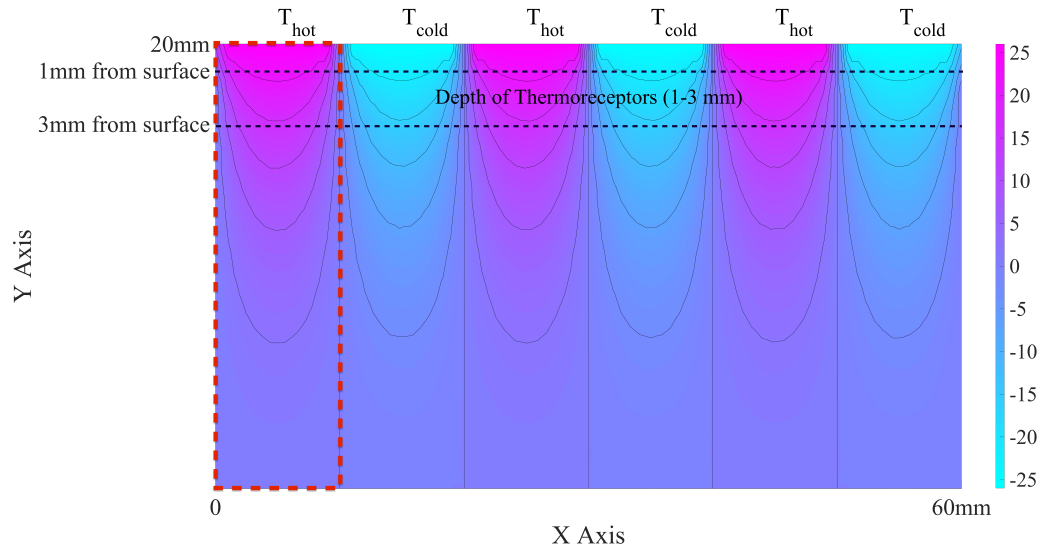
Figure 3.7: Steady state solution of the problem, when the hand is feeling the thermal grill. This has been simulated using finite element method for a mesh size of 3858×2060 over ten seconds.

The next part of the problem is to calculate the transient solution.

3.1.3   Time-dependent Solution

It is important to have all homogeneous boundary conditions in order to solve for the transient solution. We have three homogeneous boundary conditions at the two sides and the bottom. The transient solution also satisfies the full partial differential equation. $T_t = T(x, y, t) - T_{ss}(x, y) = 0$. This means that we now

36

have all homogeneous boundary conditions. We again try separation of variables

$$T(x, y, t) = f(x) \cdot g(y) \cdot h(t)$$

Putting these into the PDE, we get Equation (3.13).

$$\frac{\partial^2 T(x, y, t)}{\partial x^2} + \frac{\partial^2 T(x, y, t)}{\partial y^2} = \frac{1}{k_{finger}} \frac{\mathrm{d}T(x, y, t)}{\mathrm{d}t} \tag{3.13}$$

Similar to the method we used in the steady state solution, the left side is a sum of functions in two independent variables and the right side is a function of a third independent variable. For these two sides to be equal, the left side functions have to equal to constants and the right side function has to be equal to a constant which is the sum of these two constants.

$$\frac{1}{f(x)} \frac{\mathrm{d}^2 f(x)}{\mathrm{d}x^2} = A$$

$$\frac{1}{g(y)} \frac{\mathrm{d}^2 g(y)}{\mathrm{d}y^2} = B$$

$$\frac{1}{h(t)} \frac{\mathrm{d}^2 h(y)}{\mathrm{d}t^2} = A + B$$

Now we need to find the eigenvalues A and B.

$$\frac{\mathrm{d}^2 f(x)}{\mathrm{d}x^2} = A f(x), \qquad f(0) = f(a) = 0$$

$$\frac{\mathrm{d}^2 g(y)}{\mathrm{d}y^2} = B g(y), \qquad g(0) = g(b) = 0$$

$$A_n = -(\frac{n\pi}{a})^2, \qquad\qquad f_n(x) = \sin\left(\frac{n\pi x}{a}\right), n = 1, 2, 3, ...$$

$$B_m = -(\frac{m\pi}{b})^2, \qquad\qquad g_m(y) = \sin\left(\frac{m\pi y}{b}\right), m = 1, 2, 3, ...$$

Now we can solve for the time dependence.

$$\frac{\mathrm{d}T}{\mathrm{d}t} = k_{finger}(A_n + B_m)T$$

$$= -k_{finger}\left((\frac{n\pi}{a})^2 + (\frac{m\pi}{b})^2\right)T$$

$$T_{n,m}(t) = C_{n,m}e^P$$

$$\text{where } P = -k_{finger}\left((\frac{n\pi}{a})^2 + (\frac{m\pi}{b})^2\right)t$$

We can see that as $t \to \infty, T \to 0$. This part is the time dependent transient solution, which dies off at large values of time. So now, for any integer pair (n,m), we have the solution,

$$f(x) \cdot g(y) \cdot h(t) = C_{m,n}\sin\left(\frac{n\pi x}{a}\right)\sin\left(\frac{m\pi y}{b}\right)e^{-k_{finger}\left((\frac{n\pi}{a})^2+(\frac{m\pi}{b})^2\right)t} \qquad (3.14)$$

$$T_t(x,y,t) = \sum_{n=1}^{\infty}\sum_{m=1}^{\infty} C_{n,m}\sin\left(\frac{n\pi x}{a}\right)\sin\left(\frac{m\pi y}{b}\right)e^{-k_{finger}\left((\frac{n\pi}{a})^2+(\frac{m\pi}{b})^2\right)t} \qquad (3.15)$$

Now applying the initial condition,

$$T_0 - T(x,y) = \sum_{n=1}^{\infty}\sum_{m=1}^{\infty} C_{n,m}\sin\left(\frac{n\pi x}{a}\right)\sin\left(\frac{m\pi y}{b}\right)$$

We can make the following substitution to get the equation in a standard form.

$$v_n(y) = \sum_{m=1}^{\infty} C_{m,n}\sin\left(\frac{m\pi y}{b}\right)$$

We now find $T_0 - T_{ss}(x, y)$ in terms of this.

$$T_0 - T(x, y) = \sum_{n=1}^{\infty} v_n(y) \sin\left(\frac{n\pi x}{a}\right)$$

$$v_n(y) = \frac{2}{a} \int_0^a \mathrm{d}x (T_0 - T(x, y)) \sin\left(\frac{m\pi y}{b}\right)$$

$$C_{n,m} = \frac{2}{b} \int_0^b \mathrm{d}y v_n(y) \sin\left(\frac{m\pi y}{b}\right)$$

And then we can compute $C_{n,m}$ by putting them together.

$$C_{n,m} = \frac{2}{b} \int_0^b \mathrm{d}y \sin\left(\frac{m\pi y}{b}\right) [T_0 - T(x, y)] \frac{2}{a} \int_0^a \mathrm{d}x \sin\left(\frac{n\pi x}{a}\right) \tag{3.16}$$

3.2   Simulations

The given transient heat diffusion problem has been solved numerically us-
ing FEM software by simulating the heat diffusion problem over the specified
domain. Evaluating the analytical solution given in 3.1.2 and 3.1.3 would be a
more straightforward way to do this but it is much more convenient to simulate
the problem and obtain a solution rather than computing the given integrals.
The evolution of the solution to this problem at different time steps has been
given in Figures (3.8-3.12). The color bars at the right of the figures indicate the
color-temperature relationship. While plotting this solution, a set value of $\pm 25°$C
was used for the boundary conditions as T_{hot} and T_{cold} respectively. A mesh of
3858×2060 was used for the simulations. The simulation was run for ten seconds

and solutions were plotted for 50 frames. The two dashed black lines in the Figures (4.7-4.13) show the depth of the thermoreceptors in the hand, which lie at the lowest level of the epidermis and the highest levels of the dermis. This depth is between $1 - 3$ mm from the surface of the palm, which is the part of the hand we used in our experiment.

Simulation running time	10 seconds
Number of frames	50
Mesh size	3858×2060
Depth simulated	20 mm
Temperature at top boundary	$\pm T_{hot} = \pm 25°$C
Temperature at other three boundaries	$0°$C

Table 3.4: Specifications for the simulation run in FEM software
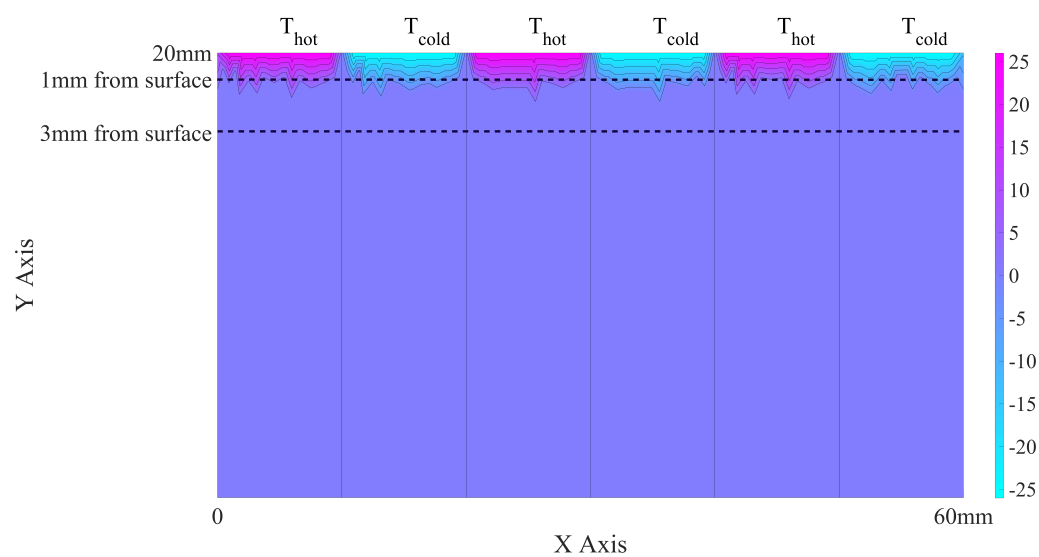
Figure 3.8: Transient solution at time (t) = 0 seconds, for problem posed in 3.1.3.

The dashed black lines indicates the depth of the epidermis, which is $1 - 3$ mm.
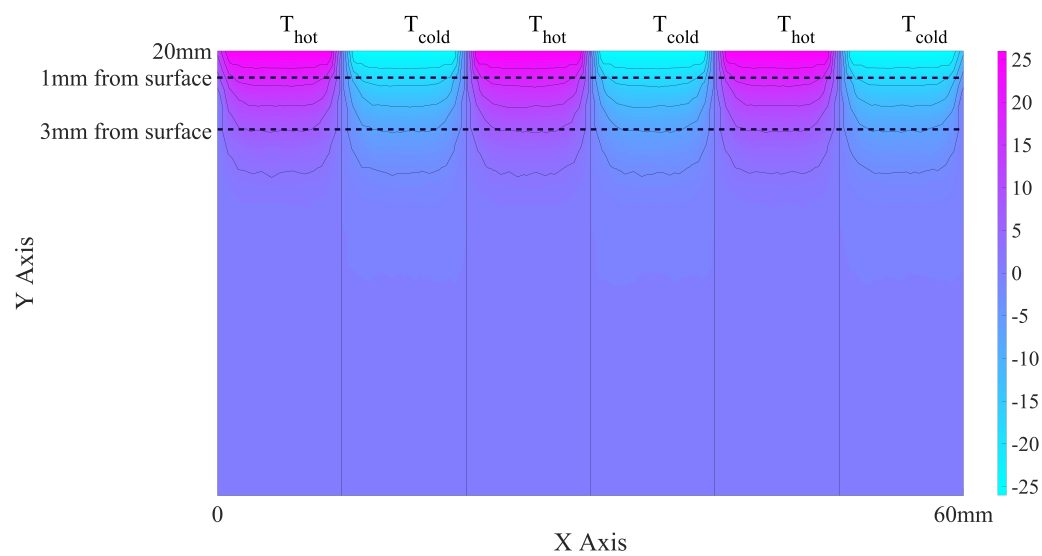
Figure 3.9: Transient solution at time (t) = 1 seconds, for problem posed in 3.1.3.

The dashed black lines indicates the depth of the epidermis, which is $1 - 3$ mm.
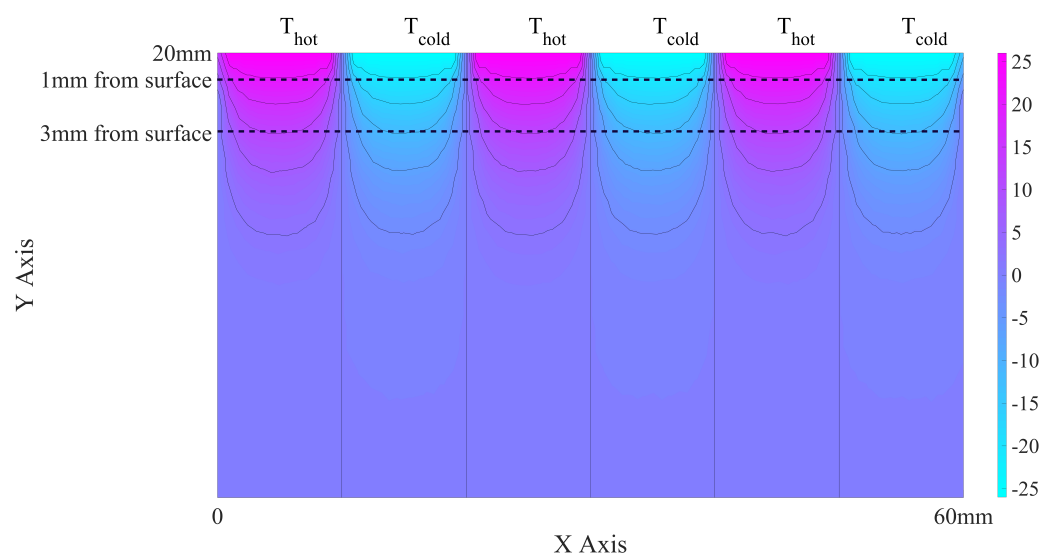
Figure 3.10: Transient solution at time (t) = 3 seconds, for problem posed in 3.1.3.

The dashed black lines indicates the depth of the epidermis, which is $1 - 3$ mm.
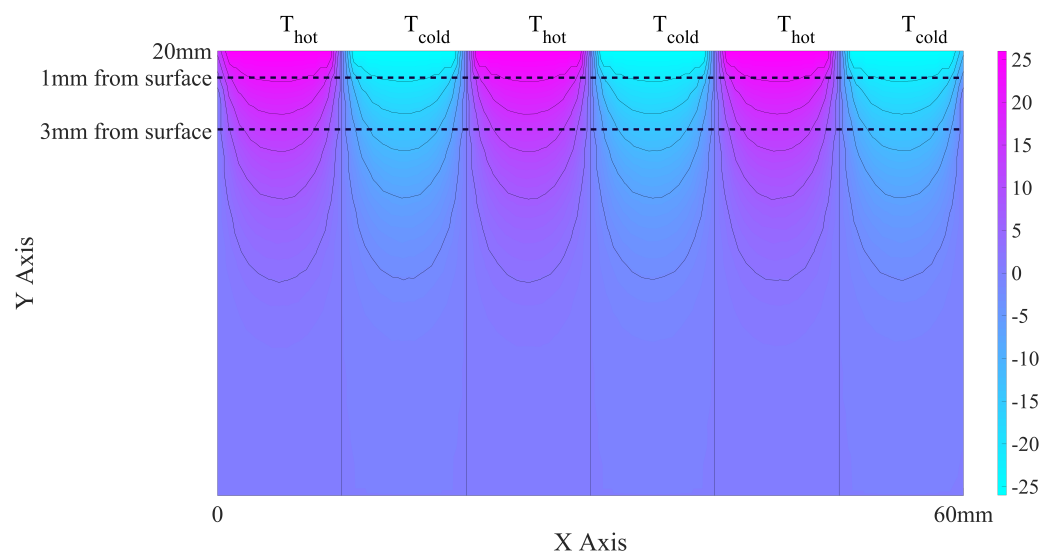
Figure 3.11: Transient solution at time (t) = 6 seconds, for problem posed in 3.1.3.

The dashed black lines indicates the depth of the epidermis, which is $1 - 3$ mm.
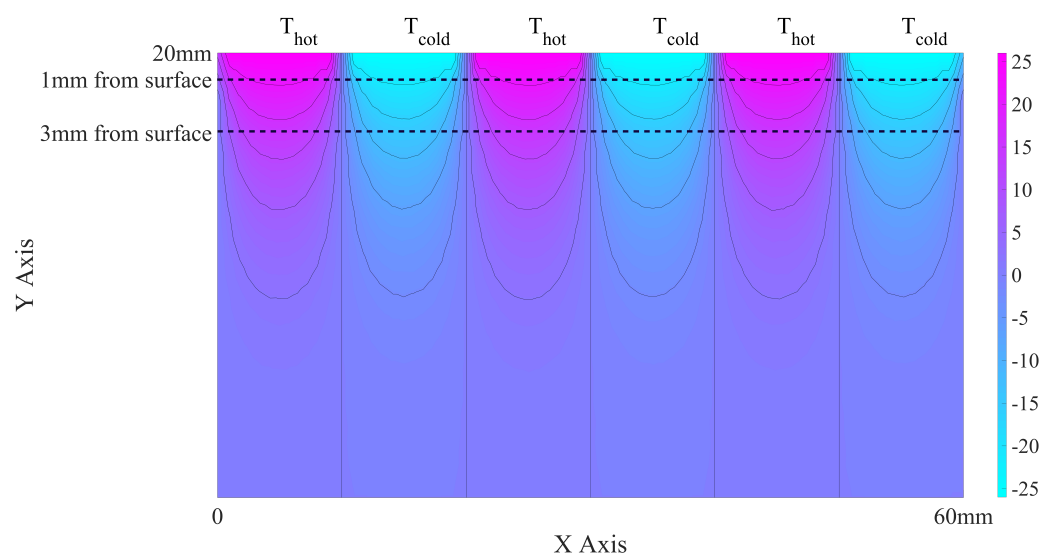
Figure 3.12: Transient solution at time (t) = 10 seconds, for problem posed in 3.1.3. The dashed black lines indicates the depth of the epidermis, which is $1-3$ mm.

Chapter 4

Quantitative Assessment of Perceptual Response Elicited by Thermal Grill

Attribution and Permissions

The contents of Chapter 4 are a work in progress by Shriniwas Patwardhan, Anzu Kawazoe and Yon Visell, in preparation for submission as a future publication. It is reproduced here with the permission of UCSB.

Shriniwas Patwardhan and Anzu Kawazoe reviewed the literature and implemented the experimental system. Shriniwas Patwardhan ran the experiment and

prepared the figures and the manuscript. Anzu Kawazoe carried out the statistical analysis, made the figures and contributed text for this chapter from some prior work. Yon Visell supervised the research, planned the experiments, and edited the manuscript

Preface to Chapter 4 : Significance for the Thesis

Chapter 4 describes an experimental study that investigates the response of participants to the thermal grill at various temperature settings. This chapter describes the experiment, methods and results. The experimental results indicate a strong dependence of the strength of the thermal grill illusion on the temperature difference between the warm and cool bars. Chapter 4 also gives a preliminary comparison between the experimental results with the spatiotemporal results given by the previously proposed model in Chapter 3. We compute the absolute gradient of temperature in the horizontal direction at a set depth inside the hand and a time instant given by response time data from our experimental results, at each temperature setting. We then compare these gradients at different temperature settings

4.1   Introduction

In this study, we assess the haptic illusion called the 'thermal grill illusion', which is felt while touching a spatially alternating pattern of warm and cool stimuli. Though these temperatures are not individually too high or too low to feel painful, touching the thermal grill made using these same temperatures feels burning hot. We use a custom thermal grill setup made up of alternating cool and warm bars. Prior work suggests a variety of theories trying to explain the thermal grill illusion. The first explanation was put forth by Thunberg [39] where he argued for a 'fusion' of cold and hot pain, in the brain. Later, Craig and Bushnell's disinhibition theory [12] has been widely accepted, in which the reduction of inhibition induced by the cold channel exposes (or unmasks) the cold-sensitive activity, thereby evoking the burning hot pain felt when touching the grill [11].

The thermal grill illusion can be a useful tool as it provides a thermal stimulus which gives an illusion of pain without subjecting the skin to extreme temperatures.

Bouhassira and others [6] showed that the intensity of the paradoxical painful sensation evoked by the thermal grill was related to the magnitude of the cold-warm differential. This indicates that the thermal grill illusion is not a digital phenomenon but has a gradient affected by the difference between the warm and

cool temperatures being felt. Just like while touching an extremely hot or cold object, the response to the thermal grill can be quantified using two observations - the intensity perceived by the person and the time taken by the person to respond to the thermal grill. A stronger thermal grill illusion, just like any other stimulus, should elicit a quicker response than a weaker stimulus. We can then examine this data and find a relationship between the temperature differential and the response time (time taken by a person to remove their hand from the thermal grill because of a burning sensation) of the person. A quantitative assessment of response times with relation to different temperature differential settings of the thermal grill has not been carried out before.

In this experiment, we measured the participant's responses (response time and perceived intensity) as they felt the thermal grill stimuli, in order to quantify the effect produced by the thermal grill.

4.2   Methods, Apparatus and Procedure

During the experiment, subjects felt the thermal grill at various temperature settings and their responses were recorded. The settings of the thermal grill were changed between trials.

4.2.1   Methods

Participants felt configurations of the thermal grill, consisting of different combinations of temperatures for the warm and cool bars, and responded indicating what they felt. We also recorded response times during the experiment. The participants felt the thermal grill at the minimum and maximum settings prior to the experiment.

4.2.2   Participants

A total of 10 subjects were initially recruited, five female and five male. This was a single site study. They were all 18 years or older, their age ranging from 22-29. They were never previously diagnosed with any type of nervous condition that could impair the normal functioning or sensing of their hands. All of them listed their right hand as their dominant hand. All subjects gave informed consent, and the experiments were approved by the institutional ethics review board of UCSB.

4.2.3   Apparatus
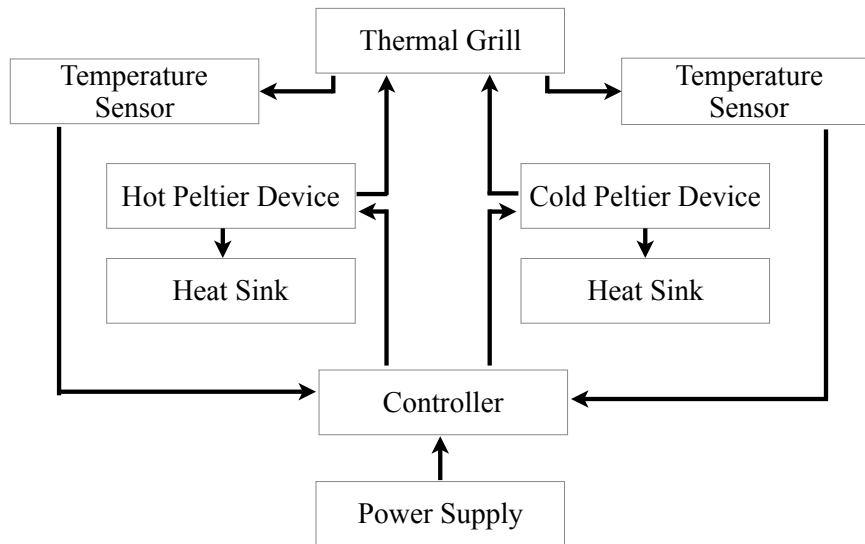
Figure 4.1: System diagram showing the experimental setup used in our study

The thermal grill surface is made of aluminum bars, each having dimensions $6 \times 6 \times 15$ mm. A total of 6 such bars are used. They are separated by 6 mm between them and arranged in an alternating pattern. Half the bars are heated from one side and the remaining half are cooled from the other side.
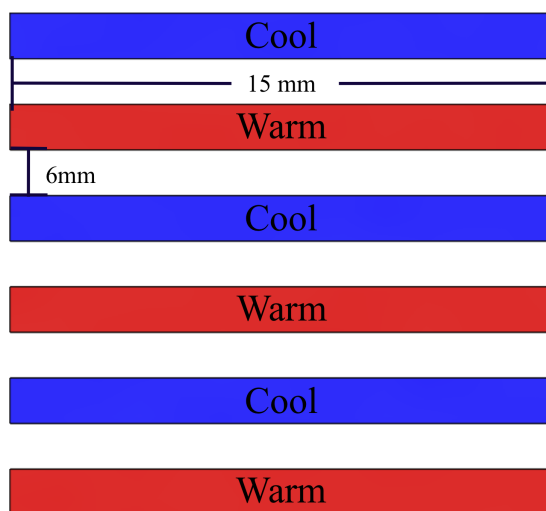
Figure 4.2: Thermal grill illustration with specific dimensions used in the study
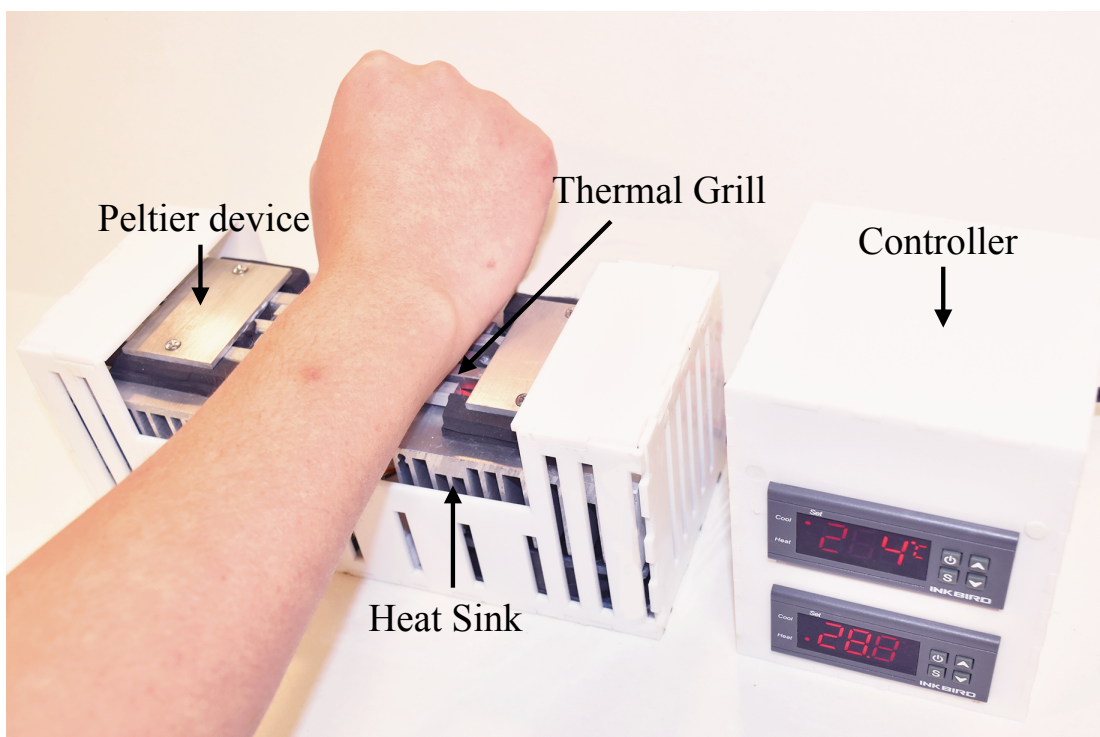
Figure 4.3: The thermoelectric haptic device used for the experiment

The heating and cooling is done using Peltier devices (TEC1-12706 Thermo-electric Peltier Cooler 12 Volt, 92 Watt). The Peltier coolers are thermoelectric devices which move heat energy from one side to another when an electric potential is applied across its terminals. Naturally, one side becomes hot and the other side becomes cold. We used heat sinks to keep one of the two sides of the Peltier devices at room temperature and thereby get a cooler or heater at the other side. We use this cold or hot side to heat or cool the aluminum bars respectively.

The voltage supplied to the Peltier devices is controlled via a computer program. The computer sends the commands to the microcontroller, which then controls the voltage applied across the terminals of the Peltier device. There are temperature sensors mounted on the aluminum bars to measure the temperature of the thermal grill components. Using this control method, the temperature of the warm and cool bars is set at the right value for each trial in the experiment.

We measured the response time of the participant using a tact switch, which records the time between being pressed and being released. This was placed under the hand of the participant and got engaged only when the thermal grill was being felt.

4.2.4   Procedure

This study is designed to assess the perception of thermal grill illusion. Prior to the experiment, the participants were asked to touch the thermal grill at the maximum and minimum temperature differential, and then rate each trial accordingly. The total duration for each participant was 1 hour including a three minute break time between each section. This break time was also required by the thermal grill to heat or cool to the new setting. The experiment was automated using software and a microcontroller.

Upon arriving at the site, participants were informed that they were taking part in a 'touch biomechanisms study'. They were asked to read the explanation accompanying the consent forms and sign them. The researcher was responsive to any questions from participants, but no such help was ultimately needed. All participants were notified that they could leave the study at any time. In addition, subjects were informed that only members of the research team would have access to their data from the experiment, and that the experimental data would be rendered anonymous and handled in accordance with the appropriate data handling procedures. Prior to the experiment, participants completed a short survey collecting anonymous demographic and screening information. The survey questions asked for the participants' gender, age, dominant hand and their previous

diagnosis of any disorder that would affect their ability of movement or sensation in their hands.
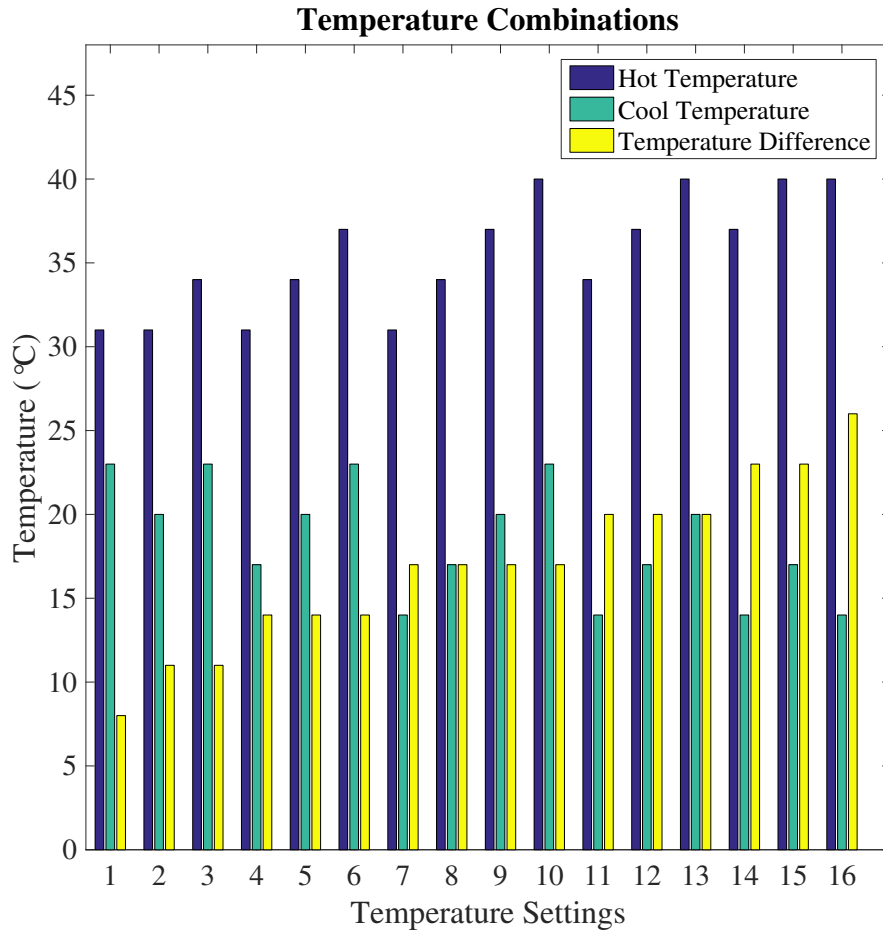
Figure 4.4: Temperature Settings for the thermal grill used in the study. Hot temperatures were varied between $31 - 40°$C and cold temperatures were varied between $14 - 23°$C. Four combinations each for hot and cold temperatures give 16 thermal grill settings. The thermal grill was set at one of these settings at each trial and each trial was repeated three times in a consecutively

They performed the experiment in a neutral environment with no distractions. Participants completed a brief guided training phase before they proceeded to the main part of the experiment. Participants were seated at a desk equipped with a computer interface and the thermal grill.

We measured their response time, as the time between when participants placed their hand on the apparatus and then removed it. After they removed their hand, the they were asked to estimate the thermal intensity on a slider scale ranging from 0-1. The minimum value (0) and maximum value (1) corresponded to the minimum and maximum temperature differential setting that the participants were allowed to feel before the experiment. This describes one trial. There were three such trials for each temperature setting. After the participant completed block of three trials, they were asked to wait for thee minutes while the thermal grill changed the temperature setting, and the process was repeated. There were a total of 16 stimulus parameter settings, see Figure (4.4).

The computer program that performs the recordings was completely automated, and provided automated prompts as to when the thermal grill should be felt in each experimental condition.

All the data was anonymized as it was stored. Statistical analysis of the anonymized data was performed in software in order to determine the correspon-

dence if any, between touch response and temperature settings. Participants were compensated with \$10 for their participation.

4.3   Results

We performed a linear regression on the data we collected for response time and perceived intensity.

As temperature difference increased by 1°C, the response time decreased by 0.506 seconds on average. With $p < 0.01$, this result was significant at the 1 % level. The R^2 value was 0.892, showing that 89.2 % of the variation in response time could be explained by a variation in temperature difference. The 95 % confidence interval was $(-0.548, -0.463)$ showing that there is 95 % probability that the population mean of the relationship between temperature difference and response time was between a decreased response time of 0.463 seconds and a decreased response time of 0.548 seconds. In other words, there was 95 % probability that in the whole population, a 1 second increase in temperature difference results in a reduced response time of between 0.463 and 0.548 seconds.

As temperature difference increased by 1°C, the perceived intensity increased by 0.0460 on average. With $p < 0.01$, this result was significant at the 1 % level. The R^2 was 0.962, showing that 96.2 % of the variation in perceived intensity could be explained by a variation in temperature difference. The 95 % confi-

dence interval was $(0.043, 0.048)$ showing that there was 95 % probability that the population mean of the relationship between temperature difference and the perceived intensity was between an increased intensity of 0.0438 and an increased intensity of 0.0482. In other words, there was 95 % probability that in the whole population, a 1 second increase in temperature difference results in an increased intensity of between 0.043 and 0.048 seconds.

Figure (4.5) indicates that as the temperature difference between the warm and cool bars increases, the perceived intensity of the thermal grill also increases. On the other hand, Figure (4.6) indicates that as the temperature difference between the warm and cool bars increases, the response time (time between keeping the hand on the thermal grill and removing it because of a burning sensation) decreases. This suggests a strong time dependence of the strength of the thermal grill illusion.

The relationship between the median of perceived intensity at each setting and the temperature difference given in Figure (4.5), was more linear than the relationship between the temperature difference and response time. This was consistent with the findings of Bouhassira and others [6], that the strength of the thermal grill illusion depends on the cold-warm differential rather than the individual cool and warm temperatures. As compared to the response times at the same temperature difference, the perceived intensity showed much less variation.
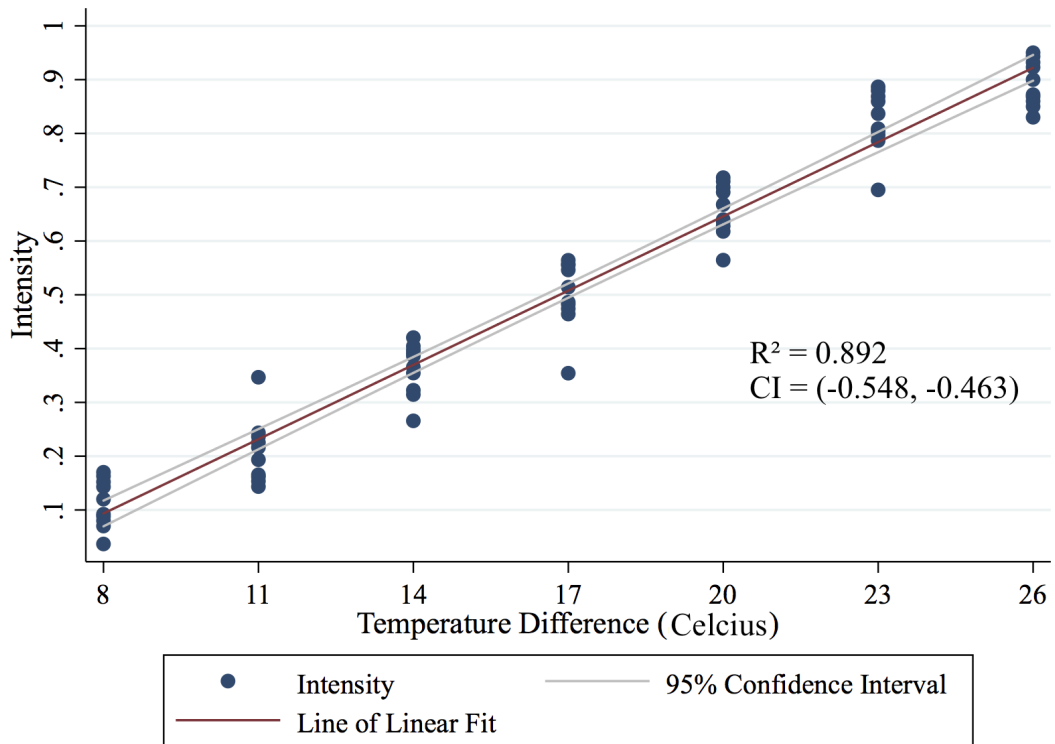
Figure 4.5: The horizontal axis represents the temperature differential of the thermal grill. The vertical axis represents the perceived intensity, from 0-1, rated against a minimum and maximum temperature differential felt before the experiment. The grey lines give the 95 % Confidence interval plot for perceived intensity and the blue dots show the actual data points. The perceived intensity shows a linear relationship with the temperature differential. R^2 was 0.892 and CI was $(-0.548, -0.463)$
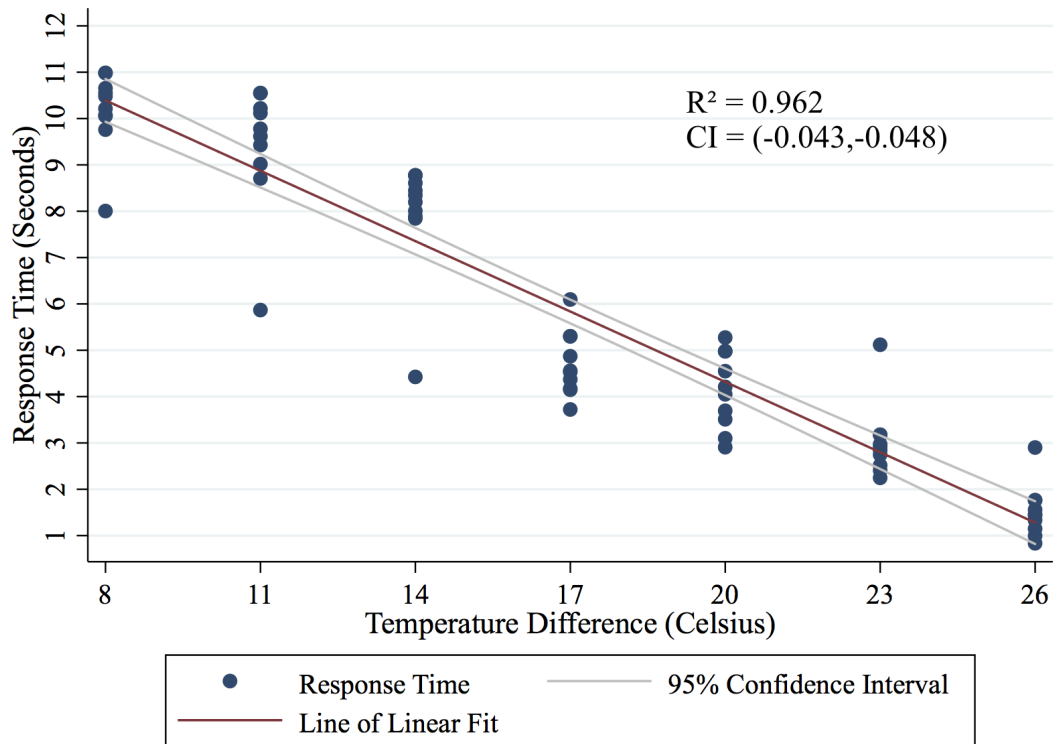
Figure 4.6: The horizontal axis represents the temperature differential of the thermal grill. The vertical axis represents the response time in seconds, measured as the time taken between keeping and hand on the thermal grill and taking it off due to a burning sensation. The grey lines give the 95 % Confidence interval plot for the response time and the blue dots represent the actual data points. Response Time R^2 was 0.962, and CI was $(-0.043, -0.048)$

The response time given in Figure (4.6), showed a quadratic relation to the temperature difference. At high temperature difference of $23-26°$C, the response times varied only between $0.5-3$ seconds while they varied between $3.5-6$ seconds

and $4.2 - 9$ seconds in the moderate $(17 - 20°\text{C})$ and between $8 - 11$ seconds $6 - 11$ seconds high $(11 - 14°\text{C})$ temperature differential range.

4.4   Preliminary Synthesis of Results from the Experiment with Model Predictions

Equations (3.12), (3.15) and (3.16) give the spatiotemporal solution to the heat diffusion problem posed in chapter 3. We can compute the value of $T(x, y, t)$ at any given depth (y) and horizontal distance (x) relating to the hand, at any time (t) by plugging these three values into the given equations. The heat diffusion problem was solved numerically using FEM software by simulating over the domain and boundary conditions given in chapter 3. The absolute value of gradient of temperature in the horizontal (x) direction was computed. We used the values of depth (y) to be between $1 - 3$ mm, the depth of the epidermis in the skin. The thickness of the epidermis varies for each body part. In our experiment, we had used the palm, and the thickness of the epidermis in the palm is between $1 - 3$ mm (one of the thickest in the human body). The epidermis in the palm has 5 layers. The most superficial layer is called *stratum corneum*, which is the most surface layer and is normally $0.2 - 2$ mm thick [26]. This is followed by the *stratum lucidium*, *stratum granulosum*, *stratum spinosum* and *stratum basale*. The

thermoreceptors are based in the last layers of the epidermis and the first layers of the dermis [19]. The thickness of the entire epidermis may be $0.8 - 1.4$ mm on the hand and soles of the feet [1]. The gradient was calculated at a conservative estimate of $1 - 3$ mm depth.

While the above description tells us the depth to examine, the time instant is given from our experimental data. So, to test our model, we compute the response at these values of depth and observed time instants. Each of these computations gave us the temperature along the horizontal (x) direction at a given time instant and depth. Then we compare the absolute value of gradients at those depths and time instants to the each other.

Temperature Difference	Time Instant
8	10
11	9.5
14	8
17	4.5
20	4.2
23	3
26	1.5

Table 4.1: Temperature Differences and time instants used for Figures

These are just preliminary results to provide a quantitative account of the TGI based on the modeling results of Chapter 3 and perceptual experiment results from Chapter 4. As we can see from Figure (4.8,4.10,4.12,4.14), a maximum absolute temperature gradient of $0.02 - 0.06°$C caused a burning sensation in the participants. These results show that a temperature differential which results in a higher temperature gradient across the domain of the hand at the set depth (location of thermoreceptors), might cause a burning sensation and offer a new window of investigation into the assessment of the thermal grill illusion. This preliminary result points us in the direction of future work which could be carried out in this regard. The response time shows a possible relationship with the gradient achieved at the depth of thermoreceptors. This could be probed further by examining if there is a small range of gradients to which the thermoreceptors react.

As described earlier, the model used to calculate this temperature response does not take into account a number of factors such as blood perfusion or internal heat sources. Further investigation is required.

Figure 4.7: Temperature $T(x)$ at a depth of 1 mm and time $1.5 - 10$ seconds at temperature difference of $8 - 26°$C. The time instants were chosen as the mean time taken by the participants corresponding to the temperature differences used in the experiment.
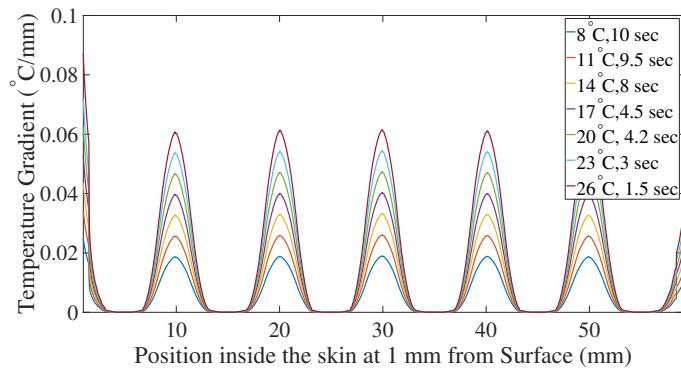
Figure 4.8: Absolute temperature gradient $\frac{\mathrm{d}T}{\mathrm{d}x}$ at a depth of 1 mm and time $1.5-10$ seconds at temperature difference of $8-26°$C. The time instants were chosen as the mean time taken by the participants corresponding to the temperature differences used in the experiment.
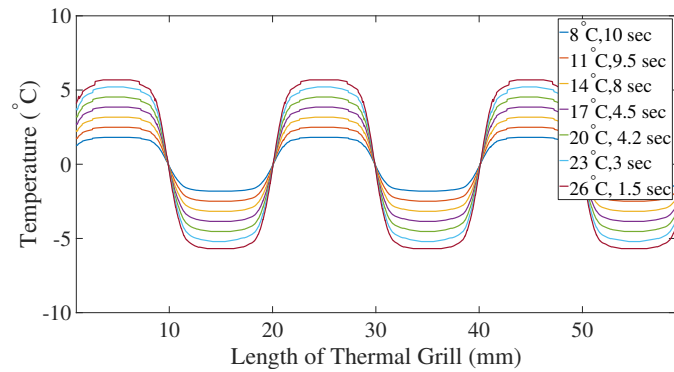
Figure 4.9: Temperature $T(x)$ at a depth of 1.5 mm and time $1.5 - 10$ seconds at temperature difference of $8 - 26°$C. The time instants were chosen as the mean time taken by the participants corresponding to the temperature differences used in the experiment.
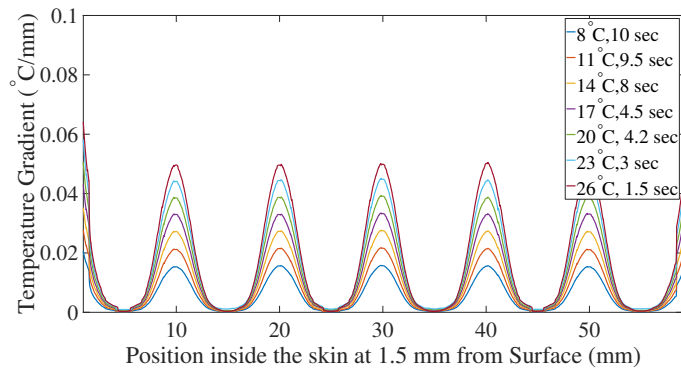
Figure 4.10: Absolute temperature gradient $\frac{\mathrm{d}T}{\mathrm{d}x}$ at a depth of 1.5 mm and time $1.5-$ 10 seconds at temperature difference of $8 - 26°$C. The time instants were chosen as the mean time taken by the participants corresponding to the temperature differences used in the experiment.
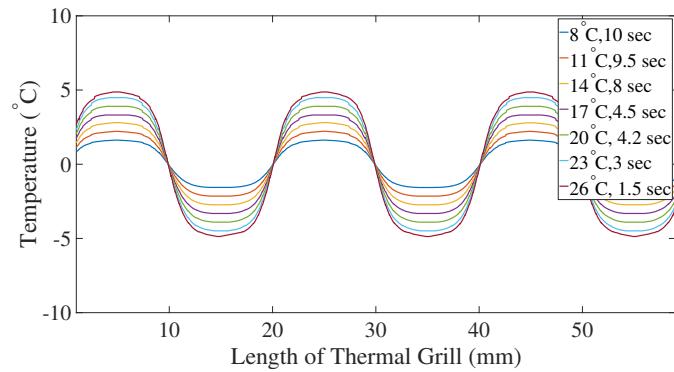
Figure 4.11: Temperature $T(x)$ at a depth of 2 mm and time $1.5 - 10$ seconds at temperature difference of $8 - 26°$C. The time instants were chosen as the mean time taken by the participants corresponding to the temperature differences used in the experiment.
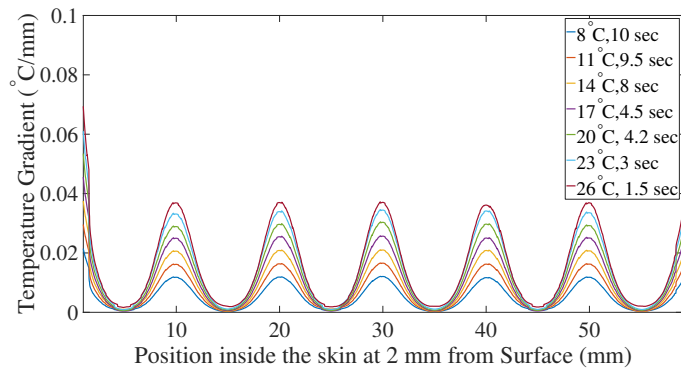
Figure 4.12: Absolute temperature gradient $\frac{\mathrm{d}T}{\mathrm{d}x}$ at a depth of 2 mm and time $1.5 - 10$ seconds at temperature difference of $8 - 26°$C. The time instants were chosen as the mean time taken by the participants corresponding to the temperature differences used in the experiment.
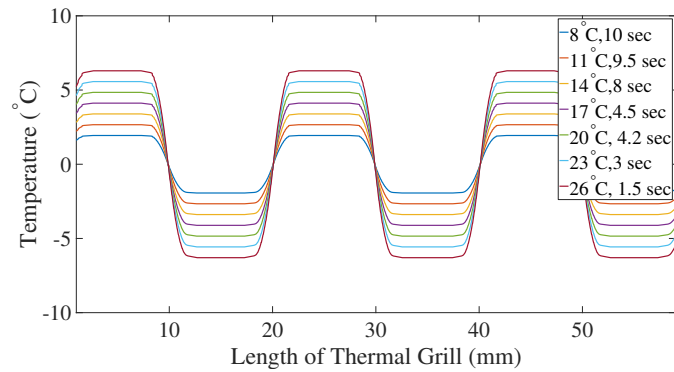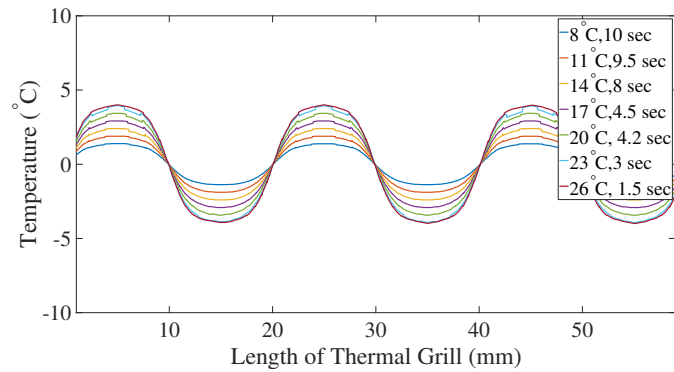
Figure 4.13: Temperature $T(x)$ at a depth of 3 mm and time $1.5 - 10$ seconds at temperature difference of $8 - 26°$C. The time instants were chosen as the mean time taken by the participants corresponding to the temperature differences used in the experiment.
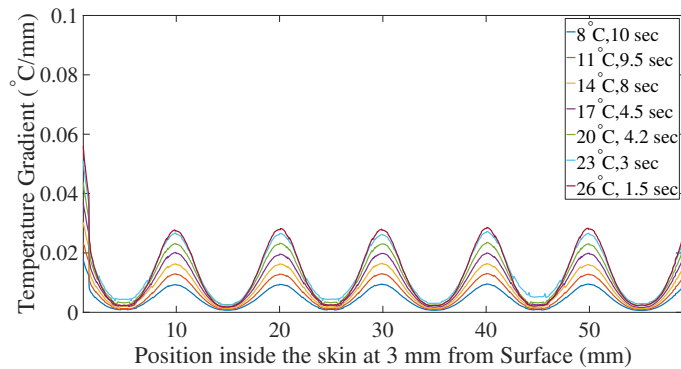
Figure 4.14: Absolute temperature gradient $\frac{\mathrm{d}T}{\mathrm{d}x}$ at a depth of 3 mm and time $1.5 - 10$ seconds at temperature difference of $8 - 26°$C. The time instants were chosen as the mean time taken by the participants corresponding to the temperature differences used in the experiment.
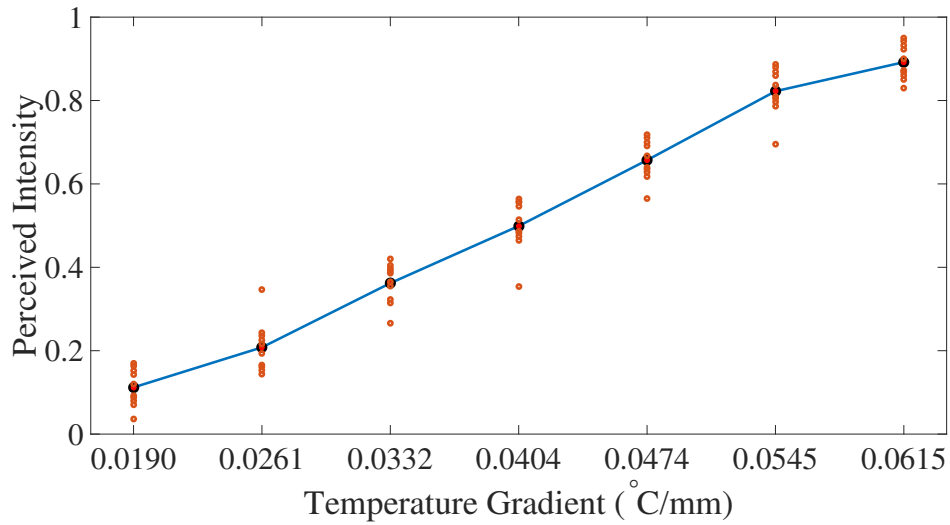
Figure 4.15: Mean of perceived Intensity of each participant (from experimental data) vs absolute temperature gradient $\frac{\mathrm{d}T}{\mathrm{d}x}$ at a depth of 1 mm for temperature difference of $8 - 26°$C. This shows that the perceived intensity increases as the temperature gradient increases, which might offer an explanation for the effect elicited by the thermal grill.

4.5   Conclusions

In this study, we measured the temporal response of the body to the thermal grill illusion. The results revealed an inverse variation in response time with respect to the temperature differential of the thermal grill.

The results show that at different temperature settings, a burning sensation is evoked at different time instants. These time instants are inversely related to the

temperature differential. The time-dependence of thermal pain shows that thermal pain is not a digital occurrence but it has a more proportional nature. The relationship between temperature differential and perceived intensity has been documented before. Though a similar relationship between the temperature differential and the response time might seem intuitive, it has not been studied before and is an important finding.

A higher magnitude of temperature differential gave rise to a quicker response time. A preliminary comparison was carried out between the results of the experiment and the model proposed earlier. It showed a possible relationship between the temperature gradient reached at the depth of the epidermis, to the response evoked by the thermal grill. This is a preliminary comparison and was performed between the modeling results of Chapter 3 and the perceptual experiment results of Chapter 4. Further work is needed.

In summary, these results may refine our understanding of the thermal grill illusion in particular and thermal pain in general, by illustrating the time-dependent nature of thermal pain in the event of touching a thermal grill.

Chapter 5

Conclusion

In this thesis, we proposed a time-dependent thermodynamic model to account for heat exchange in the skin upon touching the thermal grill and examined the temporal relationship between the temperature settings of the thermal grill and the effect elicited by it using modeling and experimental techniques. A detailed background for the thermal grill illusion and thermal displays was provided in Chapter 2. Chapter 3 proposed a thermal model to explain the thermal grill illusion. We split the problem into two parts - steady state and transient, and then proposed a solution for each of them. The heat diffusion problem was solved analytically and numerically and the solutions were discussed in chapter 3. Chapter 4 described the experimental study carried out to validate our model described in chapter 3. We asked the subjects of the experiment to feel the thermal grill

at various temperature settings and recorded their responses. These were the response time and perceived intensity. A preliminary comparison was carried out between the modeling results of Chapter 3 and the perceptual experiment results of Chapter 4. Further work is needed. Chapter 5 examines the main findings of the thesis and lists the conclusions from them.

This thesis proposes a thermal model for describing the interaction between the human skin and the thermal grill. In order to capture the time-dependent behavior of the heat transfer in the skin upon touching the thermal grill, we proposed a transient solution given in chapter 3. A number of assumptions were made in the consideration of the model. We assumed that the thermal conductivity of the human body to be isotropic from the surface to the other end of the hand, and we assumed this to be equal to the thermal conductivity of the skin. The human hand is a complex structure made up of numerous layers but incorporating all these different layers is highly complex. We also neglected the heat transfer between the part of the hand under consideration and other parts of the body through blood perfusion.

We conducted a human subject experiment, as given in chapter 4, in order to evaluate the time-dependence of the thermal grill illusion. The collected data included the participant's response time and the perceived intensity of the thermal grill. We computed the absolute gradient of the temperature ($|\frac{\mathrm{d}T}{\mathrm{d}x}|$) in the

horizontal direction at the depth of the thermoreceptors in the hand. In order to compute this, we chose the time instant at any temperature setting as the mean of the response time at that temperature setting, derived from our experimental data. We carried out some preliminary comparison of the modeled and experimental results in chapter 4 and showed that the different gradients calculated are quite close to each other and hence show that this gradient might play an important role in thermal perception, in addition to the information about the absolute value of temperature we touch.

We observed time-dependence in the results as a function of the temperature difference between the warm and cool bars. This suggests that we can possibly test for touch sensory deficits by exposing the skin to various temperature settings of the thermal grill and measuring the person's response time.

5.1   Summary of Contributions

The novel aspects of this thesis involve the study of response time to the thermal grill illusion. Thermodynamic modeling provided a framework to predict the response elicited by the thermal grill. The perceptual experiment results were compared to the modeling results and a preliminary comparison could be conducted. The main contributions of this thesis are as follows.

1. Design, fabrication and implementation of a thermal haptic display, called the thermal grill. This device is capable of setting the temperatures of the thermal grill at the desired levels. It is also capable of measuring the participant's response time to the thermal grill illusion. The measurement of response time to the thermal grill illusion is a novel contribution of this thesis.

2. Formulation of a thermodynamic model describing time-dependent interaction between the thermal grill and the cutaneous body tissues and development of analytical and numerical solutions describing the thermodynamics of body tissues stimulated by a thermal grill.

3. Comparison of perceptual responses to the thermal grill illusion recorded during the experiment to the predicted thermodynamics of tissue heating.

4. Experimental study investigating the effect of temperature differential of the thermal grill on the response elicited by it. Specifically, we measure and investigate the dependence of response time on the temperature difference, in order to compare with the time-variation of temperature gradients predicted by the thermal model.

5.2 Future work and Applications

The experiment showed that the thermal grill illusion can be used to elicit a burning sensation and that this sensation can be quantified in terms of the response it elicits. We can use the response time of the participant for this. As described earlier, we would like to investigate the possibility of detecting neuropathy using TGI. Our experiment was a study conducted on healthy participants. The next steps in order to investigate assessment of neuropathy using TGI will include a clinical study on neuropathy patients. The results of our experiment could serve as a motivation for the proposed study.

The thermal grill elicits a burning sensation without the person actually touching a very hot object. We can think of the pain induced by the thermal grill as a 'virtual' pain sensation because of the lack of actual interaction with a hot object. The temperature of the skin at the point of contact never goes below the cold threshold of pain or above the hot threshold of pain and yet the person feels burning hot while touching the grill.
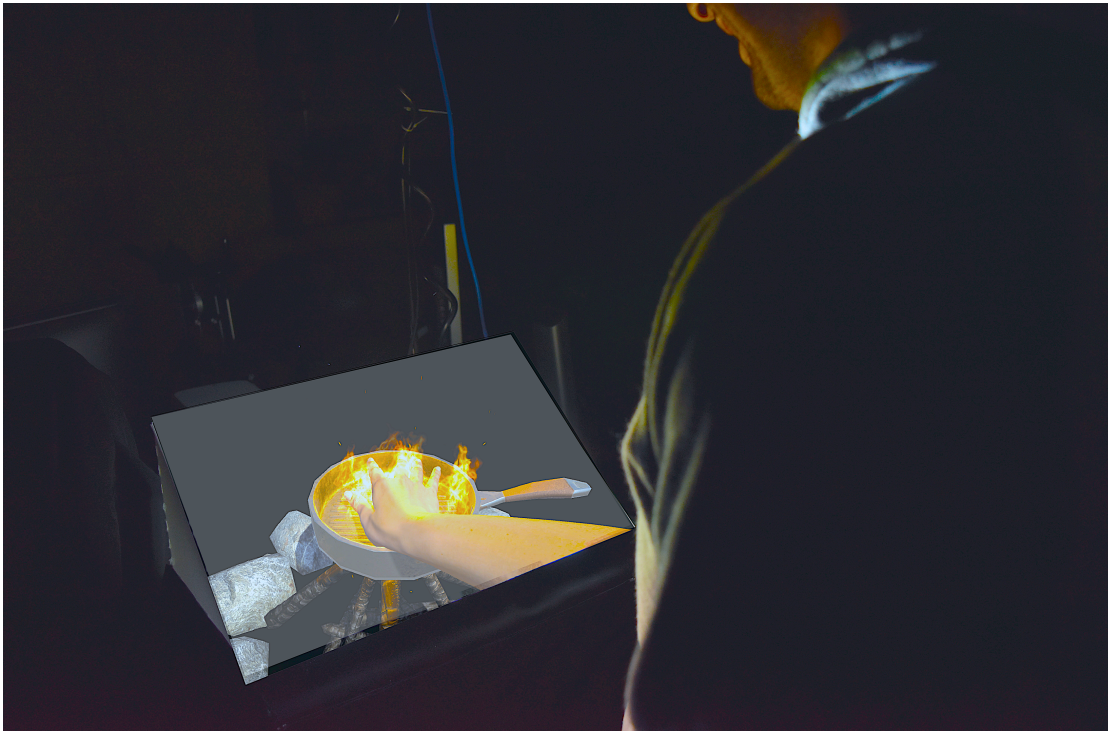
Figure 5.1: Virtual reality concept for using thermal grill illusion, by Anzu Kawazoe. It projects a 'hot' pan onto the screen and a thermal grill is placed in the position where the pan is perceived to be kept. The person then puts his hand under the screen to try and touch the hot pan but touches the grill instead, and feels a burning sensation. This opens up new avenues for VR integration of TGI

This property makes it ideal for use in VR experiences. An example would be a VR experience in which a person can touch an object like a hot pan. The participant can be asked to touch the hot pan with their hands, kept inside of a black box. The thermal grill can take the place of the virtual pan in the real world.

The thermal grill has an advantage that it can be incorporated into a number of form factors. This will enable system designers to have a variety of applications.

Bibliography

[1] Anatomy atlases: Atlas of microscopic anatomy.

[2] Patrick Bach, Susanne Becker, Dieter Kleinböhl, and Rupert Hölzl. The thermal grill illusion and what is painful about it. *Neuroscience letters*, 505(1):31–35, 2011.

[3] M Benali-Khoudjal, Moustapha Hafez, J-M Alexandre, Jamil Benachour, and Abderrahmane Kheddar. Thermal feedback model for virtual reality. In *Micromechatronics and Human Science, 2003. MHS 2003. Proceedings of 2003 International Symposium on*, pages 153–158. IEEE, 2003.

[4] Edwin Garrigues Boring. *Sensation and Perception in the History of Experimental Psychology by Edwin G. Boring.* Appleton-Century-Crofts, 1942.

[5] Matthew Botvinick and Jonathan Cohen. Rubber hands 'feel' touch that eyes see. *Nature*, 391(6669):756, Feb 19 1998. Copyright - Copyright Na-

ture Publishing Group Feb 19, 1998; Last updated - 2012-11-14; CODEN - NATUAS.

[6] Didier Bouhassira, Delphine Kern, Jean Rouaud, Emilie Pelle-Lancien, and Françoise Morain. Investigation of the paradoxical painful sensation (illusion of pain) produced by a thermal grill. *Pain*, 114(1):160–167, 2005.

[7] Andrew JM Boulton, Arthur I Vinik, Joseph C Arezzo, Vera Bril, Eva L Feldman, Roy Freeman, Rayaz A Malik, Raelene E Maser, Jay M Sosenko, and Dan Ziegler. Diabetic neuropathies. *Diabetes care*, 28(4):956–962, 2005.

[8] OpenStax College. *Anatomy and Physiology*, OpenStax CNX. `http://cnx. org/contents/14fb4ad7-39a1-4eee-ab6e-3ef2482e3e22@8.81`.

[9] A. D. Craig, E. M. Reiman, A. Evans, and M. C. Bushnell. Functional imaging of an illusion of pain. *Nature*, 384(6606):258–60, Nov 21 1996. Copyright - Copyright Nature Publishing Group Nov 21, 1996; Last updated - 2012-11-14; CODEN - NATUAS.

[10] A.D. Craig. Temperature sensation. In Larry R. Squire, editor, *Encyclopedia of Neuroscience*, pages 903 – 907. Academic Press, Oxford, 2009.

[11] AD Craig, D Bowsher, RR Tasker, Frederick Lenz, PM Dougherty, and Z Wiesenfeld-Hallin. A new version of the thalamic disinhibition hypothesis of central pain. In *Pain forum*, volume 7, pages 1–28, 1998.

[12] AD Craig and MC Bushnell. The thermal grill illusion: unmasking the burn of cold pain. *Science*, 265(5169):252–256, 1994.

[13] Ian Darian-Smith and Kenneth O Johnson. Thermal sensibility and thermoreceptors. *Journal of Investigative Dermatology*, 69(1):146–153, 1977.

[14] Leslie J Dorfman, Kenneth L Cummins, Gerald M Reaven, Joann Ceranski, Michael S Greenfield, and Leonard Doberne. Studies of diabetic polyneuropathy using conduction velocity distribution (dcv) analysis. *Neurology*, 33(6):773–773, 1983.

[15] Jeremiah John Duby, R Keith Campbell, Stephen M Setter, KA Rasmussen, et al. Diabetic neuropathy: an intensive review. *American Journal of Health-System Pharmacy*, 61(2):160–173, 2004.

[16] Eva L Feldman, MJ Stevens, PK Thomas, MB Brown, N Canal, and DA Greene. A practical two-step quantitative clinical and electrophysiological assessment for the diagnosis and staging of diabetic neuropathy. *Diabetes care*, 17(11):1281–1289, 1994.

[17] V. Ganesan and A.F. Mills. *Heat Transfer 2/E*. Pearson Education, 2009.

[18] Vincent Hayward. A brief taxonomy of tactile illusions and demonstrations that can be done in a hardware store. *Brain research bulletin*, 75(6):742–752, 2008.

[19] Herbert Hensel. Die intracutane temperaturbewegung bei einwirkung aèusserer temperaturreize. *Pflügers Archiv European Journal of Physiology*, 252(2):146–164, 1950.

[20] Hsin-Ni Ho and Lynette A Jones. Thermal model for hand-object interactions. In *Haptic Interfaces for Virtual Environment and Teleoperator Systems, 2006 14th Symposium on*, pages 461–467. IEEE, 2006.

[21] Hsin-Ni Ho and Lynette A Jones. Modeling the thermal responses of the skin surface during hand-object interactions. *Journal of Biomechanical Engineering*, 130(2):021005, 2008.

[22] Ali Israr and Ivan Poupyrev. Tactile brush: drawing on skin with a tactile grid display. In *Proceedings of the SIGCHI Conference on Human Factors in Computing Systems*, pages 2019–2028. ACM, 2011.

[23] Pedro Jimenez-Cohl, Carlos Grekin, Cristian Leyton, Claudio Vargas, and Roberto Villaseca. Thermal threshold: research study on small fiber dys-

function in distal diabetic polyneuropathy. *Journal of diabetes science and technology*, 6(1):177–183, 2012.

[24] Lynette A Jones and Michal Berris. Material discrimination and thermal perception. In *Haptic Interfaces for Virtual Environment and Teleoperator Systems, 2003. HAPTICS 2003. Proceedings. 11th Symposium on*, pages 171–178. IEEE, 2003.

[25] Lynette A Jones and Hsin-Ni Ho. Warm or cool, large or small? the challenge of thermal displays. *IEEE Transactions on Haptics*, 1(1):53–70, 2008.

[26] Lynette A Jones and Susan J Lederman. *Human hand function*. Oxford University Press, 2006.

[27] Veikko Jousmäki and Riitta Hari. Parchment-skin illusion: sound-biased touch. *Current Biology*, 8(6):R190–R191, 1998.

[28] Robert H LaMotte and Johann G Thalhammer. Response properties of high-threshold cutaneous cold receptors in the primate. *Brain research*, 244(2):279–287, 1982.

[29] Susan J Lederman and Lynette A Jones. Tactile and haptic illusions. *IEEE Transactions on Haptics*, 4(4):273–294, 2011.

[30] David Levy, Ralph Abraham, and Gordon Reid. A comparison of two methods for measuring thermal thresholds in diabetic neuropathy. *Journal of Neurology, Neurosurgery & Psychiatry*, 52(9):1072–1077, 1989.

[31] Xi Li, Laura Petrini, Li Wang, R Defrin, and Lars Arendt-Nielsen. The importance of stimulus parameters for the experience of the thermal grill illusion. *Neurophysiologie Clinique/Clinical Neurophysiology*, 39(6):275–282, 2009.

[32] Fredrik Lindstedt, Bo Johansson, Sofia Martinsen, Eva Kosek, Peter Fransson, and Martin Ingvar. Evidence for thalamic involvement in the thermal grill illusion: an fmri study. *PLoS one*, 6(11):e27075, 2011.

[33] Fredrik Lindstedt, Tina B Lonsdorf, Martin Schalling, Eva Kosek, and Martin Ingvar. Perception of thermal pain and the thermal grill illusion is associated with polymorphisms in the serotonin transporter gene. *PloS one*, 6(3):e17752, 2011.

[34] Hiromi Mochiyama, Akihito Sano, Naoyuki Takesue, Ryo Kikuuwe, Kei Fujita, Shinji Fukuda, Kenichi Marui, and Hideo Fujimoto. Haptic illusions induced by moving line stimuli. In *Eurohaptics Conference, 2005 and Symposium on Haptic Interfaces for Virtual Environment and Teleoperator Systems, 2005. World Haptics 2005. First Joint*, pages 645–648. IEEE, 2005.

[35] Gareth J Monkman and PM Taylor. Thermal tactile sensing. *IEEE Transactions on Robotics and Automation*, 9(3):313–318, 1993.

[36] Allison M Okamura. Haptic feedback in robot-assisted minimally invasive surgery. *Current opinion in urology*, 19(1):102, 2009.

[37] Harry H Pennes. Analysis of tissue and arterial blood temperatures in the resting human forearm. *Journal of applied physiology*, 1(2):93–122, 1948.

[38] David C Spray. Cutaneous temperature receptors. *Annual Review of Physiology*, 48(1):625–638, 1986.

[39] Torsten Thunberg. Förnimmelserna vid till samma ställe lokaliserad, samtidigt pågående köld-och värmeretning. *Uppsala Läkfören Förh*, 2(1):489–495, 1896.

[40] Feng Xu, Tianjian Lu, et al. *Introduction to skin biothermomechanics and thermal pain*, volume 7. Springer, 2011.